Politecnico di Torino

Politecnico di Torino

Master of Science in Energy and Nuclear Engineering

Academic Year 2023/2024

Master's Degree Thesis

Innovative Models for Hydrogen Storage: A Study on Thermal Management and Hybrid Systems

Supervisor

Prof. **Andre Lanzini**

Co-supervisors

Ph.D. **Francesco Demetrio Minuto**

Ing. **Elena Rozzi**

Candidate

Carola Bacco

Abstract

Energy storage systems are pivotal in efficiently integrating renewables into the grid for achieving a net-zero energy system. Hydrogen is increasingly recognized as a viable alternative to electric batteries for long-term and high-capacity storage. This paper presents the dynamic performance of an integrated Power-to-Power system, employing a dual approach. This involves the implementation of a hybrid storage solution that utilizes both physisorption and chemisorption, coupled with the modeling of the thermal management system.

This study builds upon prior research focused on hydrogen storage at room temperature and medium-high pressure. The extension involves expanding the hydrogen storage system model to operate at lower temperatures and pressures, aiming to increase the hydrogen storage capacity and operating conditions. The storage tank is kept at a fixed temperature through a thermal management model based on cooling cycles modeled in Aspen Hysys. Low temperatures are needed to improve the adsorption processes, while heat is applied to accelerate the release of hydrogen molecules trapped within the material. Heat is fed to the system by a heating wire.

Subsequently, this work investigates the effectiveness of a hybrid hydrogen storage system by integrating an additional chemisorption tank with the already existing physisorption tank, while maintaining original temperature and volume conditions. This hybrid approach seeks to merge the rapid response capability of physisorption with the long-term stability offered by chemisorption.

The study evaluates four different materials, including MOFs and activated carbon, and their performance compared to a simpler compressed hydrogen storage system. Findings indicate that these mate-

rials can enhance storage capacity at reduced temperatures and volumes, albeit at a higher energy cost. The dual-storage setup demonstrates that the hybrid model can improve storage capacity under constant working conditions.

In conclusion, the two innovative strategies proposed in this thesis for advancing hydrogen storage technology show promise in increasing storage efficiency but require further optimization to reduce the system's energy consumption.

Contents

List of Figures

List of Tables

1 Introduction

In the current context, the issue of the climate crisis has attracted attention. The worsening of the situation is undoubtedly evidenced by the significant increase in carbon dioxide levels in the atmosphere, which is a clear indication of an environmental crisis [1]. The current scenario can be attributed in large part to the unregulated and unrestricted use of fossil fuels in times of rapid growth. It has been observed that countries currently undergoing development phases continue to emit pollutants into the atmosphere, worsening the already considerable environmental conditions [2]. It is important to recognize that several influential institutions have taken decisive action in recent years [3], among these there are the European Union and other important powerful nations. This collaborative effort is primarily centered on dedicating substantial resources and leveraging knowledge to address this crucial issue.

In an effort to reduce high levels of carbon in the atmosphere, hydrogen has become an important energy carrier due to its superior properties and ability to produce a clean energy transition [4]. In addition to finding alternatives to fossil fuels, special attention should be paid to the development and upgrading of energy storage systems, which are another significant challenge in our modern landscape [5]. The complexities of efficient energy storage are several, not to mention the considerable cost implications associated with the development and implementation of advanced energy storage technologies. It is therefore crucial to continue to improve technology and explore different methods for efficient and sustainable energy storage.

This chapter explores the complex world of hydrogen, emphasizing its

importance in sustainable energy and its crucial role in achieving a carbon-neutral future. Additionally, it will assess different hydrogen storage solutions by examining established and emerging storage systems.

1.1 Hydrogen

Hydrogen is a promising and emerging energy source because it is abundant, renewable, and environmentally friendly. As the universe's lightest and most copious element, hydrogen is a colorless, odorless, highly flammable gas with exceptional energy content, nearly three times that of gasoline. It typically exists as diatomic gas (H_2) at standard conditions with a bond energy of 435 kJ/mol [6], but it can transform into liquid, solid, or plasma forms under specific temperature and pressure conditions (Figure 1).

While hydrogen is the most abundant element in the universe, on Earth, it is primarily found in compounds such as water and organic materials. Its production spans various energy resources, including renewable sources like wind and solar power, as well as fossil fuels, where processes in which Carbon Capture and Storage (CCS) may or may not be employed.

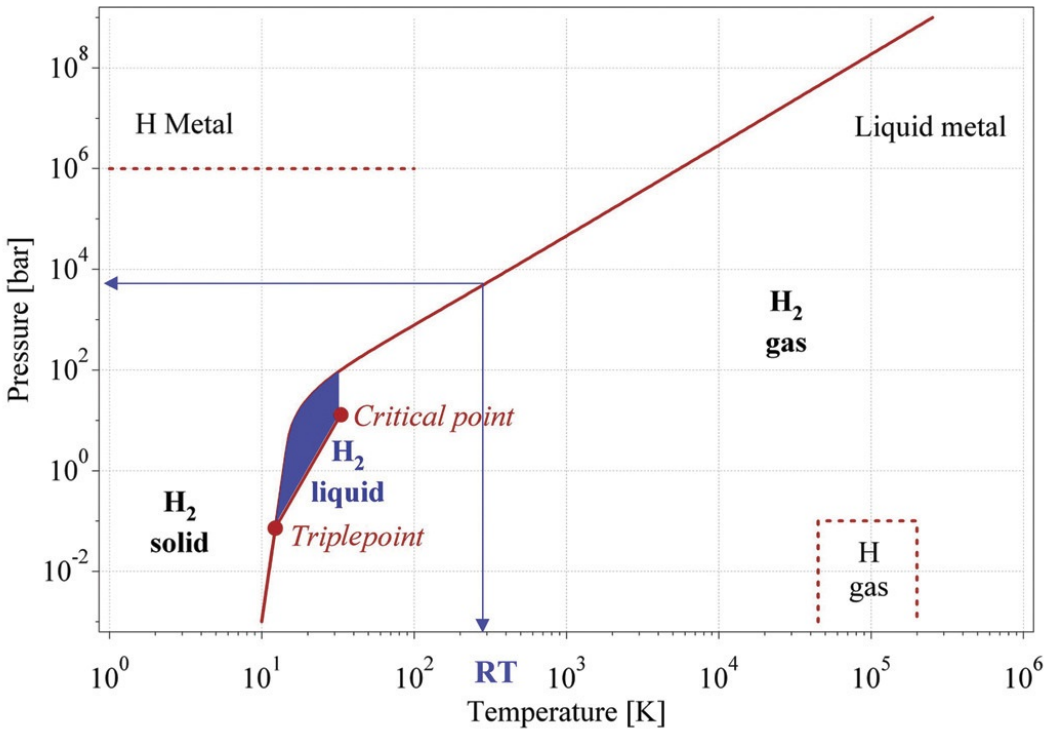

Figure 1: Phase diagram of hydrogen [7].

The versatility of hydrogen has resulted in its wide-ranging applications across various industries, including oil refining, ammonia, methanol production, and various chemical syntheses. Gaining attention as a renewable energy source, hydrogen, especially in hydrogen fuel cells, is used in vehicles by companies like GM, Daimler, BMW, Honda, and Toyota due to its higher energy density relative to volume, which makes it an ideal alternative for long-haul and heavy-duty transportation [8]. The rise of hydrogen as a pivotal element in a future economy oriented towards climate neutrality is underscored by its emissions-free applications in transportation, heating, and industrial processes, significantly contributing to environmental emissions reduction. Moreover, hydrogen plays a crucial role in

inter-seasonal energy storage, allowing energy accumulation from renewable sources during periods of abundance and its utilization when needed. Challenges persist, particularly regarding clean hydrogen's economic competitiveness compared to hydrogen produced from natural gas. However, the European Union recognizes the strategic importance of this energy vector. It is investing in research, development, and regulation to promote its use in its energy and climate policies, aiming to harness its potential to address future environmental and energy challenges.

In conclusion, hydrogen is set to play a key role in sustainable energy and the pursuit of a carbon-neutral future. From its production to its diverse applications across industries and its potential to address environmental challenges, hydrogen's importance is undeniable.

1.1.1 Properties

Some of the most significant chemical and physical characteristics of hydrogen include (Table 1):

Property	**Value**	**Unit of Measurement**
Molecular weight	2	g/mol
Density	0.08376 [9]	kg/m^3
Energy Density per unit of mass	141.9 [9]	MJ/kg
Energy Density per unit of volume	12 [10]	MJ/m^3
LFL-HFL	4-75	%
Flame adiabatic temperature	2107	°C
Auto-ignition temperature	560	°C
Diffusion coefficient in air	0.61	cm^2/s

Table 1: Hydrogen Properties.

The molecular weight of hydrogen has been extensively examined through both experimental and theoretical methods. Subsequent studies have explored hydrogen's properties under conditions of high density and pressure, offering valuable insights into its behavior across various scenarios. Hydrogen exhibits significant variations in density depending on its physical state and environmental conditions. In its gaseous form at standard temperature and pressure, hydrogen shows an extremely low density of 0.08376 kg/m^3 [9]. However, under significant compression, hydrogen can undergo a transition to either liquid or solid state, achieving respective densities of 70.8 kg/m^3 and 70.6 kg/m^3 [11]. Furthermore, when absorbed into metals or complex hydrides, hydrogen atoms can densely pack

together, exceeding these densities.

While hydrogen shows off an impressively high energy density per unit of mass, it presents a completely different profile when considered by volume. To enhance hydrogen's volumetric energy density, numerous studies have been conducted. Compression, achieved by applying high-pressure levels, stands out as a direct solution, resulting in favorable volumetric energy densities [12]. Additionally, significant effort has been made recently to address the challenge of higher energy density per unit of volume. This can be accomplished through the utilization of adsorbent materials like activated carbon or MOFs (Metal-Organic Frameworks), as well as the chemical binding of hydrogen to metal hydrides. Surprisingly, in specific contexts, these alternatives have proven to be even more advantageous than storing hydrogen in a compressed or liquefied state.

When dealing with hydrogen, it is crucial to acknowledge its particularly high flammability. Therefore, it is essential to practice meticulous care when storing and using it. Hydrogen flames ignite with remarkable speed, representing a significant hazard if not approached with the utmost caution. Additionally, performing thermal management of the system is vital, as it is necessary to avoid reaching the auto-ignition temperature. Hydrogen, due to its extremely small size, diffuses well into the crystal lattice of many metals, including iron, nickel, platinum, and palladium, while being poorly soluble in water and other solvents. This diffusion of hydrogen into the metal is responsible for the phenomenon known as hydrogen corrosion [13]. Taking these considerations into account, it becomes evident that transporting and storing hydrogen is not a straightforward task; rather, it is complex and risky. One option to consider is the safety and cost-effective transportation of hydrogen through the use of liquid organic

hydrogen carriers (LOHC). This approach allows for easy recovery of hydrogen once the destination is reached. Due to their excellent stability under ambient conditions, LOHC substances can be transported using the existing infrastructure designed for handling liquid fossil fuels [14].

1.1.2 Production

Hydrogen production is a critical aspect of the emerging clean energy landscape, and understanding the various methods of production and classifications of hydrogen is essential for shaping a sustainable future.
The produced hydrogen cannot be universally considered sustainable, indeed it can be divided into four main categories that determine its degree of sustainability [15]:

- Green Hydrogen: also known as clean hydrogen, is produced by the electrolysis of water powered by renewable electricity, no greenhouse gases are emitted during the process.
- Gray Hydrogen: is produced from natural gas by steam-methane reforming with greenhouse gas emissions.
- Blue Hydrogen: uses the same production processes as grey hydrogen, but the CO_2 is captured and stored permanently. Its production costs are more expensive than grey hydrogen but cheaper than green hydrogen.
- Turquoise Hydrogen: is produced by pyrolysis of natural gas, with pure carbon as a side product that can be sold on the market. It is still at an early stage of development but has the potential to become a cost-efficient process.

There are several methods of hydrogen production, with some being more economically advantageous than others, while some are more sustainable but less cost-effective. Currently, the dominant technology accounting for approximately 96% of hydrogen production, in accordance with the European Parliament report, involves steam methane reforming, which extracts hydrogen from natural gas or coal. While this method is cost-effective, it comes with significant carbon dioxide emissions. The alternative is to produce hydrogen through water electrolysis. However, it is important to note that at present, the capital cost of electrolyzers remains relatively high, making this approach more expensive compared to the dominant technology.

The most common methods for hydrogen production include:

- Steam Methane Reforming (SMR): a fossil fuel processing technology that transforms hydrogen-containing compounds obtained from fossil fuels into a gas stream rich in hydrogen. Steam methane reforming, presented in Figure 2, is the prevailing method, primarily because of its cost-effectiveness and high efficiency. However, it generates substantial CO_2 emissions making it important to control the H/C ratio to limit the carbon dioxide formation. To further enhance hydrogen production and reduce the carbon dioxide content, a water-gas shift reactor is typically employed after the reforming process [16]. Grey hydrogen is produced when CO_2 is released during the process, while blue hydrogen is generated when the CO_2 is captured and permanently stored.

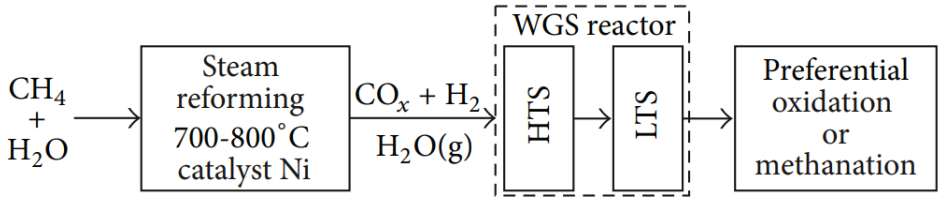

Figure 2: Steam reforming scheme.

- Electrolysis: a promising method for hydrogen production involves electrolysis, which employs water and electricity. This process accounts for 4% of the world's hydrogen demand and is a cleaner alternative because it does not produce greenhouse gases, and the oxygen generated has additional industrial applications [15]. However, it may not be considered as a primary option due to the high capital costs associated with electrolyzers and the substantial energy demands of the process. Indeed, to be cost-effective, electrolysis necessitates consistent access to low-cost electricity. In addition, when coupled with renewable electricity sources there are no greenhouse gas emissions throughout the entire hydrogen production process, resulting in the production of green hydrogen as the final product. Different electrolysis technologies could be employed for hydrogen production, including Alkaline-based, PEM (Proton Exchange Membrane), and SOEC (Solid Oxide Electrolysis Cells). Among these, PEM, shown in Figure 3, is the most developed technology, while SOEC stands out as the most efficient option.

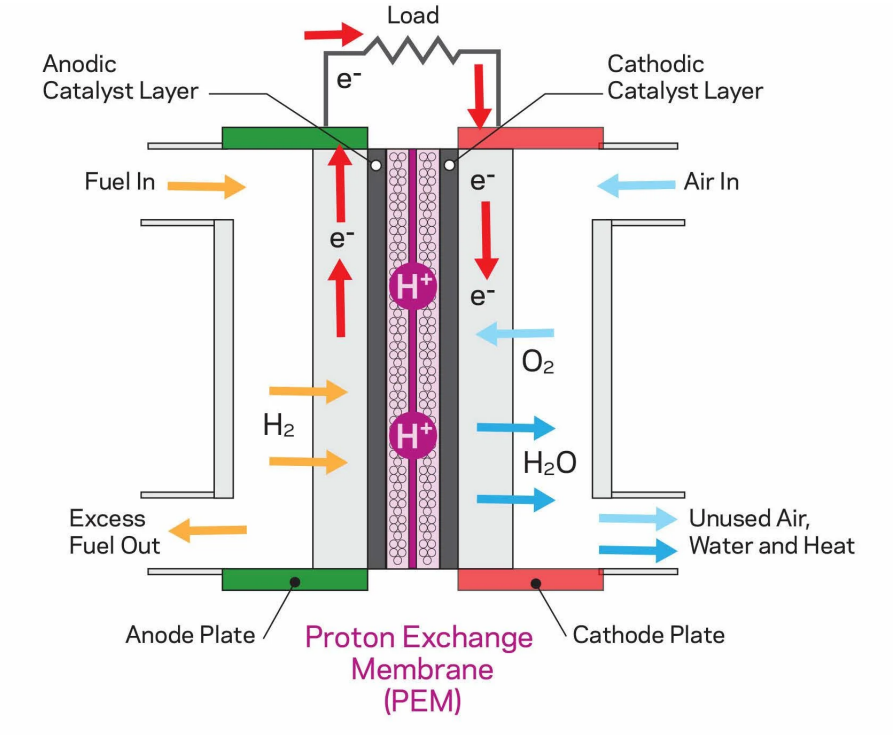

Figure 3: Proton Exchange Membrane scheme.

[17]

- Biomass gasification: a thermochemical process used to produce hydrogen. While reforming primarily involve natural gas and oil, gasification expands its application to coal. Thus this versatile method can also be exploited with different biomass sources, such as agricultural and forestry residues, energy crops, and municipal waste. In fact, biomass steam gasification converts raw biomass materials into combustible gases including hydrogen and various hydrocarbons, the process is rapresented in Figure 4. This conversion process occurs at elevated temperatures and is facilitated by introducing water vapor as a gasification agent. Gasification is widely recognized as a promising

choice for industrial production due to its higher efficiency and hydrogen yield compared to pyrolysis. However, several challenges persist, including the reduction of tar content, optimization of catalyst composition, and the reduction of both energy and material costs [16].

Figure 4: Gasification process [18].

- Photoelectrolysis: a process also known as direct water splitting, where photoelectrochemical cells are used to produce hydrogen from water using sunlight as the energy source. This approach has the potential to generate hydrogen directly from sunlight in such a way as to eliminate the need for costly components and correlated energy losses. However, it currently faces challenges in economic competitiveness compared to alternative hydrogen sources due to many technical complexities. Photoelectrolysis uses light to conduct electrolysis, then converts light into electric current to transform substances such as H_2O or H_2S into valuable energy products like hydrogen, the process is , presented in Figure 5. By integrating solar energy capture and

water electrolysis within a single photoelectrode it stands as one of the most effective renewable methods for hydrogen production [19].

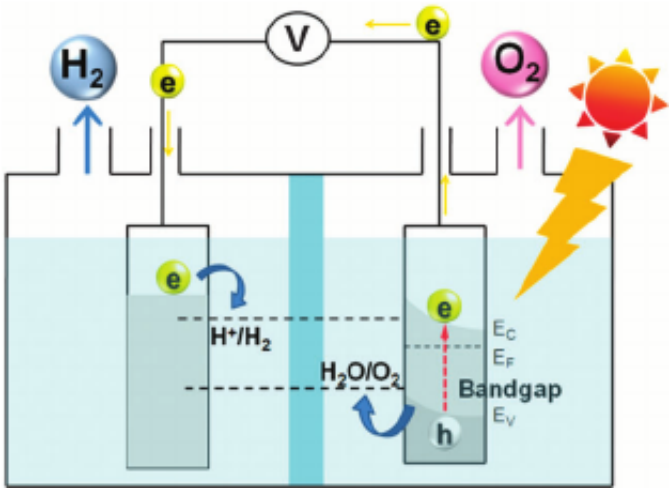

Figure 5: Photoelectrochemical cell scheme [20].

While grey hydrogen from steam methane reforming remains prevalent due to its cost-effectiveness, the transition to cleaner options like green and blue hydrogen is gaining momentum. It's important to consider not only the ecological aspect of the produced hydrogen but also the efficiency of its production.

The availability of diverse production methods enables hydrogen to be generated across a range of environments all around the world. This adaptability makes hydrogen a versatile energy carrier, capable of meeting the demands of different scenarios and applications. This solidifies hydrogen's role as a flexible and adaptable energy vector.

1.1.3 Applications

In the future, climate-neutral renewable electricity will play a dominant role, especially clean hydrogen will play a significant part in non-electrified applications such as heavy-duty transport and steel industries. Electrification will require a substantial expansion of electricity generation and grid, while hydrogen will require investment in infrastructure. Retrofitting existing gas networks can reduce the need for additional expenses. Hydrogen can also support the management of fluctuations in renewable energy sources, thus making it possible to store and convert electricity during peak demand. However, all this comes at the cost of a certain efficiency compared to the direct use of electricity. Hydrogen therefore offers a versatile range of applications in the emerging sustainable energy system, especially due to its adaptability it will be a valuable asset in many sectors. Hydrogen is used directly in fuel cells, where it serves as the primary fuel to generate electricity through a chemical reaction with oxygen. This technology has considerable versatility and finds multiple applications in different sectors. Fuel cell vehicles, such as hydrogen-powered cars and buses, make use of hydrogen fuel cells for propulsion. FCVs offer emissions-free transportation with advantages such as longer ranges and quicker refueling compared to battery electric vehicles. If hydrogen were to become the predominant fuel for future vehicles, it would be essential to plan the construction of refueling stations carefully. Currently, there are approximately 1,100 hydrogen refueling stations worldwide, with China being the leading installer, followed by Europe [21]. The annual increase in hydrogen-powered vehicles corresponds to a rise in refueling stations. The strategic placement of refueling stations is also a crucial aspect. By carefully locating these stations,

it is possible to expand and diversify the user base.

Fuel cells are also commonly employed as backup power systems, providing reliable electricity during grid outages. They play a critical role in ensuring uninterrupted power for essential infrastructure, data centers, and telecommunications facilities. The off-grid stationary power generation units also adopt this technology for on-site electricity generation in residential, commercial, and industrial settings. They not only produce electricity but also capture and exploit waste heat, enhancing overall energy efficiency. This combined heat and power (CHP) application is an efficient way to meet both electrical and thermal energy needs.

Additionally, hydrogen blending into the natural gas network is gaining attention as a means to reduce the carbon footprint of natural gas. By injecting hydrogen into the existing natural gas infrastructure, we can gradually transition toward a cleaner energy source while making use of the existing distribution infrastructure layout. This approach has the potential to decarbonize heating and cooking in residential and commercial buildings while minimizing the need for extensive infrastructure changes. However, it is important to note that some modifications to appliances may be required when hydrogen blending is implemented. Due to the high permeability of hydrogen conventional materials are unsuitable for its transportation and storage because of hydrogen corrosion. Existing gas networks are not suitable for transporting pure hydrogen in their current state, so new pipelines with suitable materials, different welding technology, compressors, sensors, and safety equipment will be required. However, it is worth noting that the use of hydrogen for domestic heating is not significant, as there are many more efficient options available. For example, electric heat pumps offer significantly higher energy efficiency compared to using hydro-

gen, as they do not involve the losses associated with energy conversion, transportation, and utilization. In addition to new applications, hydrogen also finds use in traditional industrial applications such as chemical production, including ammonia and other chemicals, as well as in electronic and metal processing. However, it's important to note that these applications typically require relatively small quantities of hydrogen. The hydrogen value chain is extensive, some of the various applications are represented in the figure 6.

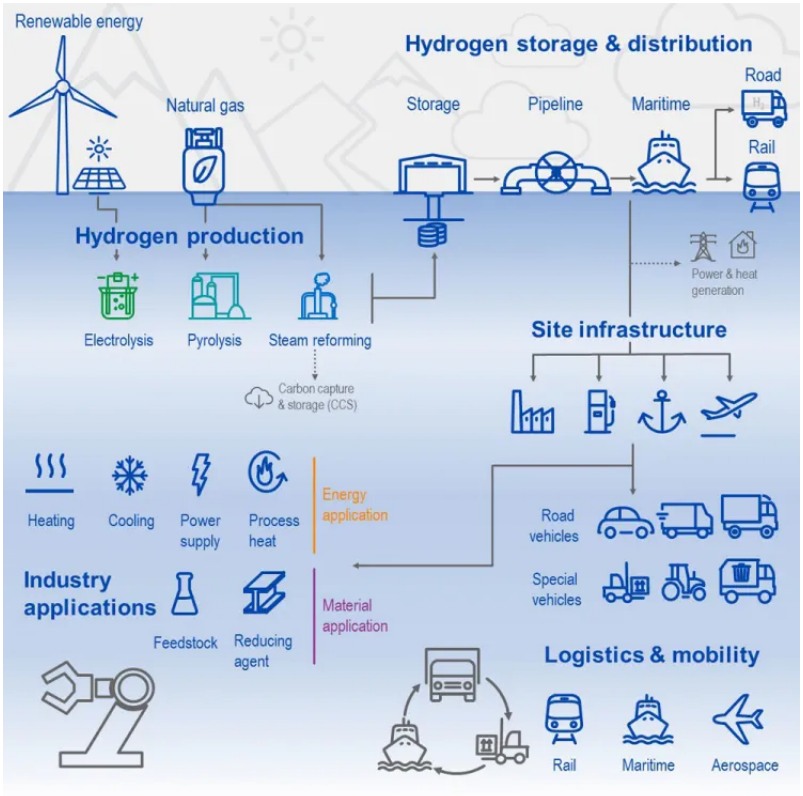

Figure 6: Hydrogen value chain [20].

1.1.4 Market Developments

The European Union has set an ambitious goal of decarbonizing energy consumption through the widespread use of electricity from renewable sources. However, renewable electricity alone may not be able to cover the entire energy demand, but hydrogen offers a solution to fill this gap. Although green hydrogen, produced from renewable sources, is not yet economically competitive compared to traditional grey hydrogen, Europe can successfully advance clean hydrogen production. This new energy vector can become increasingly relevant thanks to advancements in renewable energy technology and the urge to reduce greenhouse gas emissions. Estimating a 14% rise in hydrogen usage within the European energy mix by 2050, it is crucial to secure substantial funding, establish a comprehensive regulatory framework, explore innovative market solutions, and develop an extensive infrastructure network within the EU, in collaboration with third-party nations.

One of the key objectives for Europe is to harness renewable sources to produce hydrogen, concurrently creating job opportunities and fostering economic growth. To achieve these goals, significant investments will be required to develop electrolyzers, implement carbon capture and storage (CCS), and manage the entire hydrogen production, distribution, and storage chain. It is essential to start using hydrogen as soon as possible, even if it's not entirely sustainable, for two primary reasons: firstly, to reduce CO_2 emissions, and secondly, to initiate and promote the adoption of hydrogen as an energy source.

In 2015, the European Commission adopted a legislative proposal to revise the European Union Emissions Trading System (EU ETS), which in-

cludes the establishment of an Innovation Fund. This fund, aggregating approximately 10 billion euros, is designed to support low-carbon technologies during the 2020-2030 period. The fund can substantially mitigate risks associated with complex and large-scale projects, representing a unique opportunity to promote hydrogen technologies on a broad scale.
The strategy involves, firstly, establishing an EU investment agenda through the European Clean Hydrogen Alliance and strategic European investments under the InvestEU program (from 2021). Additionally, it will be essential to boost demand and enhance production, supported by a favorable regulatory framework and continuous technological development.

The transition plan adopted by the EU will follow a phased approach: from 2020 to 2024, the aim is to install at least 6 GW of electrolyzers in Europe to produce green hydrogen; from 2025 to 2030 at least 40 GW of electrolyzers should be installed, and hydrogen should become a significant element for the energy mix; from 2030 to 2050, renewable hydrogen technologies will be mature and exploited to decarbonize challenging sectors [22].

1.2 Energy Storage Systems

The increase in global energy consumption is closely linked to variations in the energy load profiles of end-users, whether they are private or industrial. Within the framework of the European Strategic Energy Technology Plan (SET Plan), one of the fundamental pillars revolves around decarbonization and improving the efficiency of energy resource utilization. The proposed solution to address this challenge is the widespread use of RES, which is now widely distributed and diversified. However, this approach includes some relevant issues to address. RES generates energy intermittently and not consistently, creating a fluctuating energy supply. Furthermore, a massive penetration of RES into the electrical grid can lead to significant imbalances in the system. Consequently, it becomes essential not only to reduce primary energy consumption but also to stabilize the voltage in the electrical system [23].

This is where the concept of Energy Storage Systems, becomes relevant. These systems allow for the control and minimization of fluctuations in the electrical grid caused by intermittent injections of energy from sources such as solar and photovoltaic. These systems store excess energy when it is available and make it available when the grid needs it, thus contributing to making the grid more modern, efficient, and smart. Moreover, the presence of energy storage systems significantly reduces the risk of power outages within a smart grid with distributed energy sources. All of this translates into more efficient energy management, with minimal losses and relatively low costs.

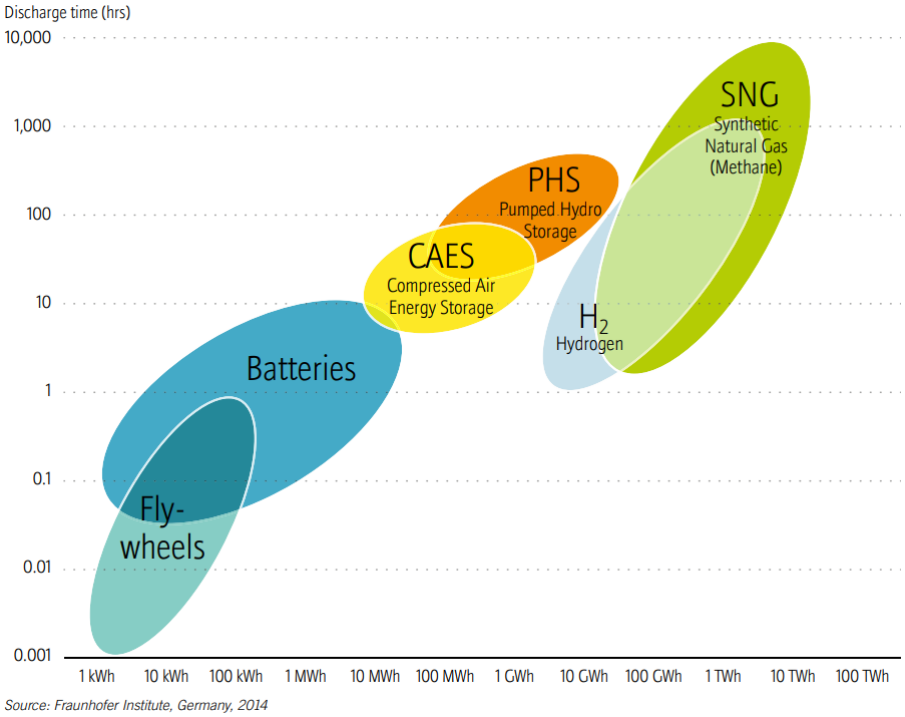

Figure 7: Overview of storage capacity of different energy storage systems [24].

There are different types of storage systems, presended in Fugure 7, which can be classified into two main categories: energy storage and power storage. Energy Storage systems are used to store energy for long periods and typically provide services with a slow release of relatively low power. Common examples of energy storage systems include batteries, compressed air energy storage (CAES), flywheels, thermal energy storage, hydrogen, and plug-in electric vehicles. On the other hand, power storage systems accumulate power for short periods but can release it quickly and immediately. These systems are designed to improve the reliability and security of the electrical grid. An example of power storage system is electrolytic capacitors and superconductors. This distinction between energy storage and

power storage is important because different types of systems are suitable for different purposes and can help address specific challenges in integrating renewable energy sources into the electrical grid. In particular, energy storage systems are critical for enabling the integration of renewable energy sources into power grids and supporting the transition to more sustainable energy systems.

1.2.1 Hydrogen Storage Systems

As mentioned in the previous section, the key points revolve around the use of renewable sources for energy production and energy storage to balance energy supply and demand, especially when dealing with intermittent RES. The latter can be achieved through hydrogen. In fact, when there is excess electricity, it can be used to power an electrolyzer, which generates oxygen and hydrogen as its products. Hydrogen can then be stored in various ways and later used to power a fuel cell, which is capable of generating electricity without emitting any pollutants, with water as its only byproduct. Alternatively, it can be used directly as a fuel source to generate heat or serve as a feedstock for industrial processes and products. The key factors for the storage system involve achieving high volumetric and gravimetric energy densities, fast charge and discharge processes, ensuring working conditions at room temperatures and atmospheric pressure, guaranteeing safety, and offering cost-effectiveness. The most relevant storage solutions are [25]:

- Compressed hydrogen storage: compressed gas is the most widely used and recognized technology for hydrogen storage. There are typically four types of pressure vessels that can be used for storing hydro-

gen due to their properties that enable safe storage without corrosion. These vessels can be categorized based on their materials, maximum allowable pressure, cost, and gravimetric density [kg_{H_2}/kg_{tot}]. An excellent choice is a type IV tank, Figure 8, which can withstand an internal pressure of 700 bar with a gravimetric density of 5.7%, as seen in the Toyota Mirai [25].

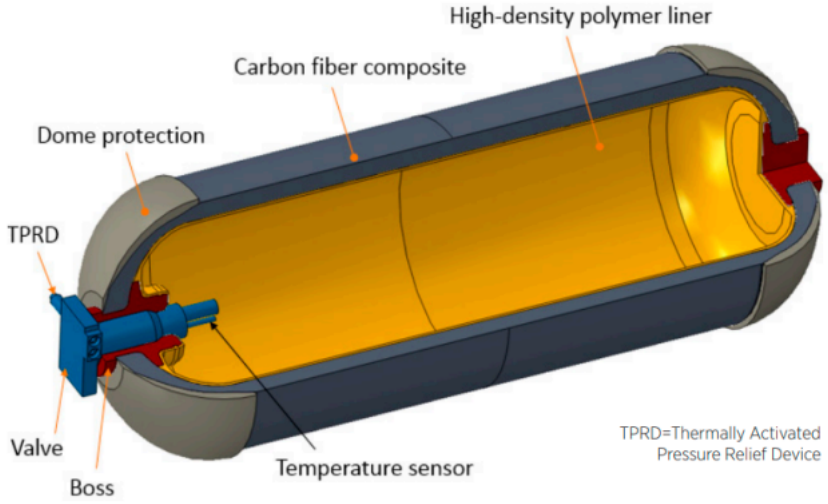

Figure 8: Type IV tank for hydrogen storage [25].

As the pressure increases, the volumetric density also increases, reaching its peak above 1000 bar. However, the gravimetric density decreases as the pressure increases, with the highest gravimetric density achieved at zero overpressure. Consequently, the gains in volumetric storage density come at the expense of reduced gravimetric density in pressurized gas systems. Gas compression is associated with the release of heat, and addressing this issue often involves pre-cooling the hydrogen gas before it is injected into storage. However, this process results in a notable energy loss. Typically, the pre-cooling sys-

tem is coupled with a membrane compressor, a device that employs semi-permeable membranes to compress gases efficiently, minimizing energy losses during the compression process. The high-pressure storage method, despite being technically simple and well-established on a laboratory scale, suffers from significant drawbacks, including the relatively low hydrogen density and the requirement for extremely high gas pressures within the system, and safety remains a major concern, especially when it is located in high density populated areas [7].

- Liquid hydrogen storage (LH_2): involves maintaining extremely low temperatures, specifically at the boiling point of hydrogen, which occurs at 21.2 K when kept at ambient pressure. Unlike compressed gas storage, the primary challenge in LH_2 storage lies in coping with cryogenic temperatures rather than high pressures. To effectively manage LH_2 storage, it is crucial to minimize heat transfer with the environment. This is achieved through the design of storage tanks with a high-volume-to-surface ratio, making spherical tanks the most suitable choice, a real example can be seen in Figure 9. Larger tanks offer advantages by reducing the rate of evaporation and lowering the required insulation mass, both of which are critical for minimizing boil-off losses caused by heat transfer. From an application perspective, LH_2 is generally unsuitable for vehicles due to the complex thermodynamics involved. However, it does hold promise for use in aircraft due to its impressive energy density. It's important to note that this technology comes with substantial costs, both in terms of energy consumption and equipment investment.

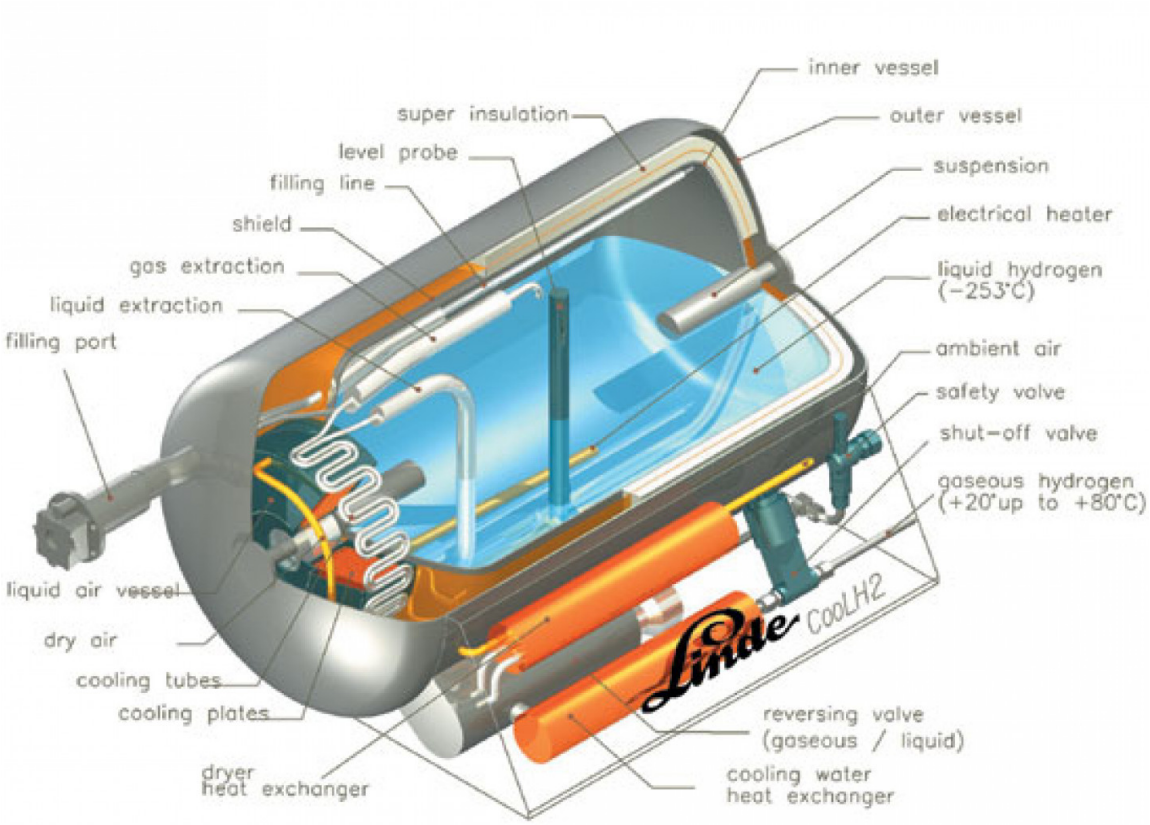

Figure 9: Liquid hydrogen storage tank [26].

- Physisorption hydrogen storage: employs materials with extremely high surface areas, such as nanoporous substances, to effectively capture and release hydrogen molecules. This method relies on the weak Van der Waals forces, enabling a fast and straightforward adsorption and desorption process. In stark contrast to chemisorption, the different nature of the processes can be seen in Figure 10, physisorption has a significantly lower binding energy, typically only a few millielectronvolts (meV), compared to the several electronvolts (eV) needed

for chemical adsorption. A key advantage of this process is its lack of requirement for activation energy to initiate the adsorption or desorption. Several theoretical models, including the Dubinin-Astakhov and Langmuir models, have been proposed to represent this phenomenon, each with its own set of assumptions and principles. Key adsorbent materials adopted for this storage method are activated carbon and metal-organic frameworks. Physisorbent materials fulfill 13 out of 16 of the US Department of Energy performance criteria, making them highly appealing study topics. However, improvements are necessary in volumetric and gravimetric capacities, as well as in minimizing hydrogen losses. Achieving optimal volumetric capacity is particularly challenging due to the difficulty in obtaining the same level of compactness observed in ideal crystal packing scenarios. Enhancing gravimetric performance is feasible by incorporating lighter atoms into the structure of the MOF [27].

The adsorption process generates heat, and if not promptly dissipated, it can significantly reduce the overall efficiency of the system. When the adsorbate transitions from the gas phase to the adsorbed phase, there is a change in molar enthalpy, and this heat component is essential for fully describing the thermal performance of the storage system. Not dissipating this heat can raise the temperature within the tank, thereby reducing the net deliverable capacity. [28] The adsorption capacity is primarily influenced by the specific surface area of the material, and it tends to decrease as the temperature increases. The total storage capacity of a porous solid combines adsorption on the solid surface with compression in the void spaces. However, physisorption

is particularly effective at low temperatures due to the weak nature of the interactions involved. In summary, physisorption offers advantages such as reversibility and rapid cycling and refilling times. However, it faces challenges like clustering issues and the need for either low temperatures or high pressures to be effective [29].

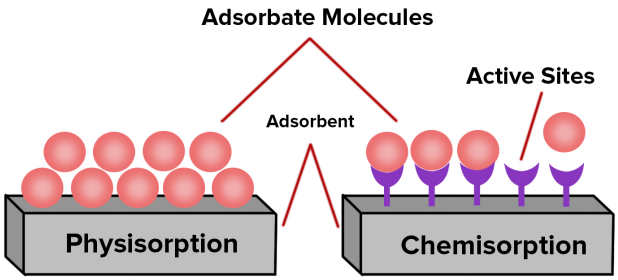

Figure 10: Differences between physisorption and chemisorption.

- Chemisorption hydrogen storage: involves chemical processes where hydrogen is both stored and released through chemical reactions. This storage type ensures high thermodynamic stability at ambient temperatures due to the strong bonding formed between hydrogen and the chemical component, while kinetic properties suggest that achieving rapid dehydrogenation kinetics still requires elevated temperatures

(over 300°C) [30]. An important consideration when utilizing chemisorption for hydrogen storage is the adsorbent material's capacity to adsorb and desorb a maximum quantity of adsorbate, which directly impacts the storage efficiency. This method uses materials such as ammonia (NH_3), metal hydrides (MH), and liquid organic hydrogen carriers (LOHCs).

Metal hydrides are capable of absorbing hydrogen and later releasing it, either at room temperature or upon heating. These hydrides form strong bonds with hydrogen, necessitating high temperatures, typically between 120°C and 200°C, to release the hydrogen. Metal hydrides selected for storage purposes are characterized by their low reactivity, safety, and their ability to achieve high hydrogen storage densities. However, they face significant drawbacks due to their violent reaction to moist air, handling, and recycling difficulties, and the tendency to absorb impurities. These impurities can reduce the lifetime of storage tanks by occupying the metal sites initially reserved for hydrogen [29].

Liquid organic hydrogen carriers are unsaturated organic compounds that can store significant amounts of hydrogen, facilitating easy transport and release under specific conditions.

Ammonia stands as the world's second most produced chemical, bringing advantage from an extensive infrastructure for its production, transport, and distribution. It features a well-developed technology base for both synthesis and distribution and is relatively easy to catalytically decompose. Ammonia can be combined with water and stored as a liquid at room temperature and pressure, offering high hydrogen

storage densities with minimal cryogenic requirements. Additionally, ammonia storage does not result in CO_2 emissions, presenting an environmental advantage [29].

In summary, chemisorption hydrogen storage offers high-density hydrogen storage solutions with the benefits of safety in metal hydrides, the capacity for significant hydrogen storage in LOHCs, and the environmental advantage of ammonia. However, challenges include the handling and recycling of metal hydrides, the need for high temperatures to release hydrogen, and the infrastructure requirements for ammonia [29].

In Table 2, the main characteristics of presented storage methods can be observed, providing valuable information for selecting the most suitable storage method according to the situation.

Parameters	**Storage Type**				**Unit**
	Compressed	**Liquid**	**Chemical**	**Physisorption**	
Gravimetric capacity ρ_m	13	Varies	≈ 18	20	%
Volumetric capacity ρ_v	≈ 40	70.8	150	20	kg m^{-3}
Temperature	273	21.5	373–573	Varies	K
Pressure	800	1	1	100	bar
System cost	12–16	6	8–16	100/60	$/kWh

Table 2: Characteristics of different types of hydrogen storage [29].

2 Methodology

The methodology chapter of this thesis builds upon the framework proposed by Rozzi et al. [31]. Building upon the insights provided by this study, the research aims to expand its findings and investigate additional scenarios in thermal management and hydrogen storage systems.

The article investigates hydrogen storage in solid materials via adsorption for stationary applications. It delves into exploring the benefits of coupling P2P plants with H_2 storage (Figure 11) in microporous adsorbent materials at ambient temperature and medium to high pressures . Consequently, the study develops a dynamic model alongside an energy management strategy, complemented by a thermal management system for electrochemical devices and the compression unit. The performance analysis of adsorption on porous materials is conducted under real operational conditions at full scale. Furthermore, the H_2 storage tank is charged during surplus renewable energy source production and emptied when RES-generated energy fails to meet the load demands. The study evaluates two configurations: one involving H_2 adsorption and mechanical compression in microporous materials, and the other solely featuring mechanical compression in an empty tank.

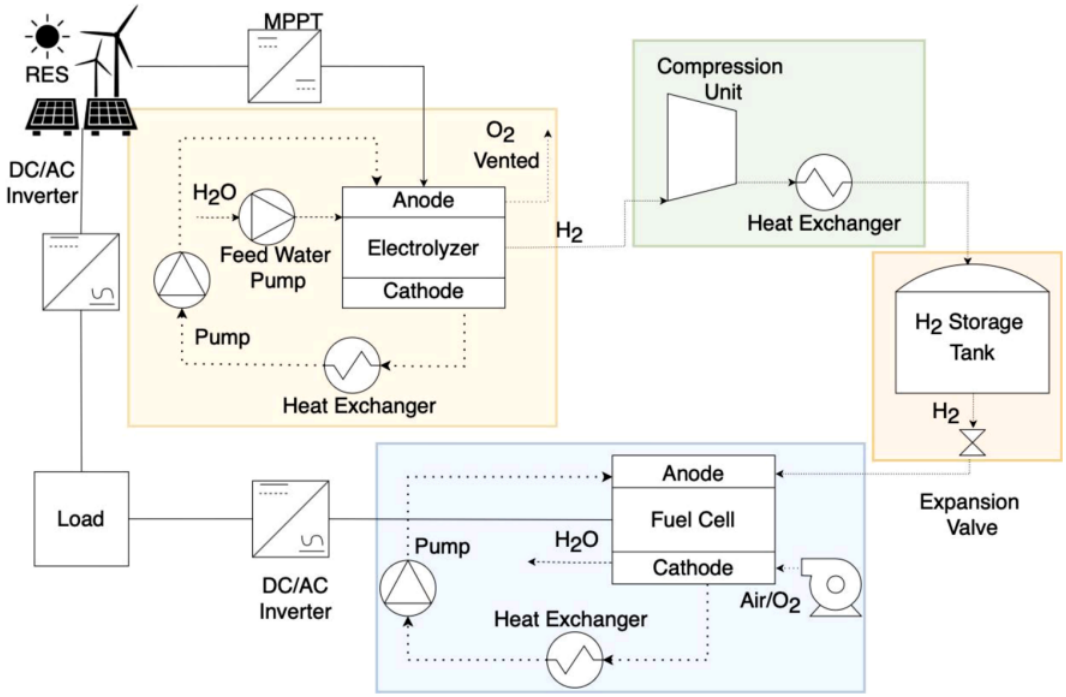

Figure 11: Schematic of the P2P system configuration [31].

The system operates as follows: electricity is generated through RES, which is then converted from alternating current to direct current. In the absence of demand from the load, surplus electricity is used to charge the hydrogen storage tank with hydrogen produced by the electrolyzer (PEMEC). However, when there is a power demand from the load, the electricity generated by the RES is directly supplied to the load. If the tank can be charged, excess electricity from the RES powers an electrolyzer, converting electricity into a useful fuel, hydrogen. The control parameters for this block include the working temperature of the electrolyzer, excess power, and the state of charge of the tank. If the hydrogen output from the PEMEC is at a lower pressure than the storage tank, the compression unit, in this case, the diaphragm compressor, operates to compress and cool the

hydrogen to the storage pressure and ambient temperature. Subsequently, when the hydrogen is in storage conditions, it is inserted into the tank. Storage discharge depends on the power requirement, level of H_2 in the storage tank, stack temperature, and the amount of H_2 recirculated from the anode side. Modified Dubinin-Astakhov equations are employed to represent the adsorption of H_2 in the tank. The investigated adsorbent materials include MSC30, IRMOF-1, NU-110, and C/Be_2. Tank filling is determined by the state of charge and the flow rate of H_2 generated by the electrolyzer. The main outputs include the round trip efficiency of the Power-to-Power plant for one charge/discharge cycle, energy supply to the electrolyzer fully converted back into electricity by the fuel cell, breakdown of energy consumption, amount of energy withdrawn from and injected into the grid, maximum storage operating pressure, and storage volume and weight.

This thesis aims to propose two different implementations of the system presented above. At first, a new thermal management of the tank is studied and added to the existing system. Then, the incorporation of a second tank is considered, transforming the model into a hybrid hydrogen storage system.

2.1 Thermal Management of the Tank

One of the key elements of the system that can be examined to get more accurate results is the hydrogen tank. In this model, presented in Figure 12, the tank is supposed to be loaded with solid materials, storing hydrogen within pores through physisorption. During hydrogen adsorption, heat is released, and conversely, during desorption, heat needs to be supplied to facilitate a faster discharge. This heat is handled through the vessel thermal management system shown in Figure 13. To understand the physics beneath the problem, it is essential to first calculate the amount of heat generated that has to be removed from the system during storage charging or the heat required by the system that has to be provided during discharge. This value depends on three parameters: the material used for hydrogen adsorption, the operational conditions of the tank (temperature and pressure), and the maximum storage capacity of the tank. Subsequently, a cooling and heating system is introduced into the model to maintain the tank at a fixed temperature, to effectively mitigate the effect of this released/required heat, defined as isosteric heat of adsorption/desorption and heat losses due to convection.

With the main aim of understanding the system's energy dynamics, one of the first objectives of this study is to comprehend the overall energy expenditure of the system. This information is crucial not only to evaluate which scenario is optimal but also to identify areas for improvement. Therefore, it is essential to study the energy balance of the tank, derived from the first law of thermodynamics, applied to the control volume, which includes only the tank. The approach adopted in this study involves treating the problem as a 0D model, ensuring uniform effects of both cooling and

heating when applied to the tank. Further investigations and optimizations are required to identify the optimal layout of the heat exchanger within the tank to ensure optimal heat exchange.

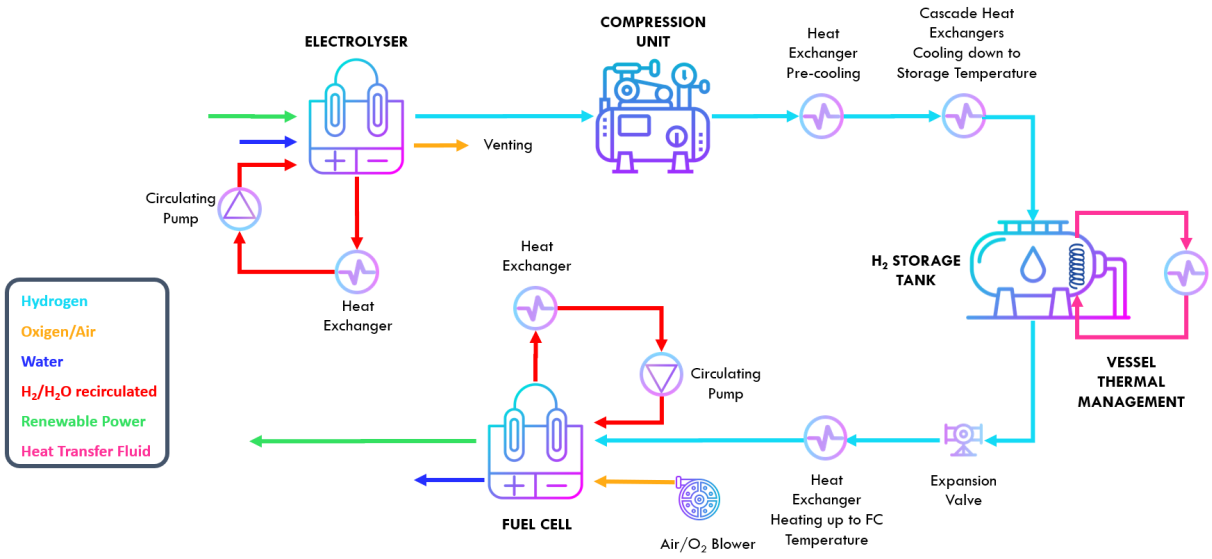

Figure 12: Energy storage system model.

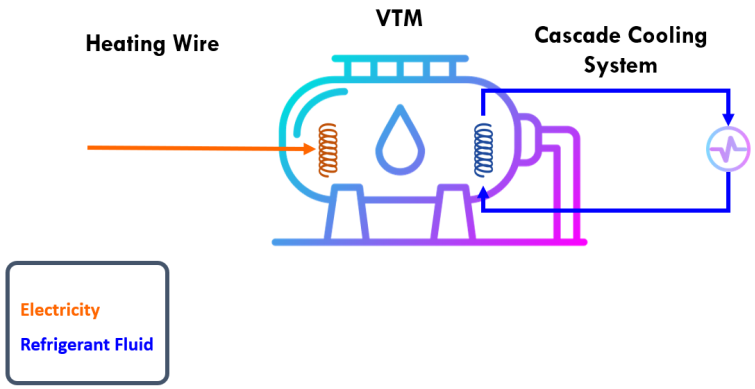

Figure 13: Vessel Thermal Management system.

The energy balance equation applied to the control volume is the following:

$$H_f - H_i = Q_l + Q_{c/h} \tag{1}$$

$$Q_{H_2,total} = Q_{c/h} + Q_{H_2} \tag{2}$$

where:

- H is the enthalpy of the system at specific conditions
- Q_l is the heat lost due to convection between the tank and the environment
- $Q_{c/h}$ is the heat that is necessary to remove or to give to the system to keep the working conditions
- Q_{H_2} is the amount of heat that needs to be either removed from the incoming hydrogen mass flow rate to bring it to the tank's operating temperature or supplied to the exiting hydrogen flow to ensure it meets the operating conditions of the fuel cell at the required temperature

From equation 1, the unknown parameter represents the amount of heat required to be removed or supplied to the control volume to maintain the tank at its working temperature. Additionally, further energy expenditure arises from heating the incoming hydrogen to the storage's working temperature and cooling it to the fuel cell's working temperature upon exit. From equation 2 we obtain the total amount of heat required by the system considering the entering/exiting hydrogen and the tank.

The system operates as follows: water is supplied to the electrolyzer at the working temperature of the electrolyzer (T= 80 °C) to prevent thermal shock to the element. Hydrogen produced exits the electrolyzer at its working temperature, also at 80°C. At this point, the outlet pressure of the electrolyzer is checked. If the pressure is below 25 bar, the hydrogen does not require compression before entering the tank. Instead, it passes only through an intercooler, which reduces the hydrogen's temperature from 80°C to the ambient temperature of 25°C before being introduced into the tank. However, if the pressure ranges between 25 and 30 bar, the hydrogen flow passes through a compressor, which compresses the hydrogen to create an overpressure of 5 bar above maximum tank pressure, enabling insertion into the tank. Once compressed, the hydrogen exiting the compressor is cooled from the compressor discharge temperature to the ambient temperature of 25°C through a water cooling stage, and the amount of heat removed is calculated according to Equation 3.

$$Q_{H_2} = n_{H_2} * C_{H_2} * \Delta T \tag{3}$$

In equation 3, during the charging phase, n_{H_2} represents the moles of hydrogen entering the tank, C_{H_2} denotes the specific heat capacity of hydrogen (28.8 J/molK), and ΔT represents the temperature difference between the incoming hydrogen and the storage's working temperature. This calculation is also applied when the hydrogen exits the tank. In the discharge scenario, n_{H_2} is the number of moles required by the fuel cell, and ΔT is the temperature difference between the storage and the fuel cell's working temperature.

The temperature difference depends on which scenario is considered.

$T_{EC} - T_{amb}$ is used to calculate 3 when the exiting hydrogen from the electrolyzer bypass the compressor unit and goes directly into the intercooler. $T_{comp,discharge} - T_{amb}$ is used in the case the hydrogen passed through the compressor unit before the intercoolig process. $T_{tank} - T_{FC}$ is used when discharging the tank to feed the fuel cell.

After the hydrogen is introduced into the tank, the energy expenditure required to cool the hydrogen to the tank's working temperature is calculated. This calculation is performed using equation 3 but considering the temperature difference between the tank and the environment.

The cooling process of hydrogen during the tank charging phase occurs in multiple steps. Initially, the hydrogen is cooled to ambient temperature, for which a water cycle is sufficient to remove the heat. However, when it comes to cooling the hydrogen inside the tank, temperatures down to -190°C are reached. Achieving this level of cooling requires a more complex technology compared to a water cycle. This system will be explained in detail in the section 2.1.3.

2.1.1 Enthalpy

The enthalpy formulation employed in this study was adapted from Peng et al. [32] to fit this scenario.

To accurately formulate the enthalpy equation at state j, it was necessary to define several parameters. Firstly, the amount of hydrogen in solid and gaseous forms was quantified in kilograms.

$$m_{\mathrm{H_2,tank}} = m_{\mathrm{H_2,solid}} + m_{\mathrm{H_2,gas}} \tag{4}$$

$$m_{\mathrm{H_2,solid}} = \frac{\eta_{\mathrm{storage}} \cdot m_{\mathrm{ads}} \cdot m_{\mathrm{excess}}}{1000} \tag{5}$$

$$m_{\mathrm{H_2,gas}} = (n_{\mathrm{H_2,storage}} \cdot MM_{\mathrm{H_2}}) - m_{\mathrm{H_2,solid}} \tag{6}$$

$$m_{\mathrm{exc}} = \left[\frac{n_{\mathrm{H_2,storage}}}{m_{\mathrm{ads}}} - (V_{\mathrm{pore}} \cdot \rho_{\mathrm{H_2}}(T,p))\right] \cdot MM_{H_2} \left[\frac{\mathrm{g_{H_2}}}{\mathrm{kg_{ads}}}\right] \tag{7}$$

Where $m_{\mathrm{H_2,solid}}$ represents the mass of hydrogen in the solid phase, and $m_{\mathrm{H_2,gas}}$ represents the mass of hydrogen in the gaseous phase. The calculation of the sorbent material quantity within the tank is determined as follows:

$$m_{\mathrm{ads}} = V_{\mathrm{tank}} \cdot \eta_{\mathrm{pack}} \cdot \rho_{\mathrm{bulk}} \tag{8}$$

- η_{storage} represents the amount of hydrogen that is absorbed compared to the theoretical limit.
- η_{pack} represents how much internal volume of the tank is occupied by the sorbent material, the remaining volume is used for equipment and heat exchangers.
- m_{excess} is the hydrogen excess uptake, this value can be obtained by fitting the hydrogen isotherms or, as in this case, with equation 7
- V_{tank} is the internal volume of the tank.
- $\rho_{\mathrm{sk}} = \frac{\rho_{\mathrm{crystal}}}{V_{\mathrm{pore}}}$ $[\mathrm{kg/m^3}]$ is the skeletal density, representing the density of the solid material and the closed pores; the fraction is between the crystal density of the sorbent material and the pore volume per unit of mass.

- $\rho_{\text{bulk}} = (1 - \epsilon_{\text{p}}) \cdot \rho_{\text{sk}}$ is the bulk density, it depends on how the material is managed.
- ϵ_{p} is the pellet porosity, in this study is set at 0.6.
- ρ_{H_2} is the density of hydrogen at a certain temperature and pressure; CoolProp library from Python is used to obtain this thermodynamic value.
- MM_{H_2} is the hydrogen molecular weight.

In this study, a value of 1 has been assumed for both η_{storage} and η_{pack} efficiencies. All these parameters were useful to obtain the mass of hydrogen, expressed in equations 6 and 5, used in equation 9 that represents the total enthalpy expressed in kJ.

$$\begin{aligned} H_j = {} & m_{\text{H2,solid}} \cdot \left[\Delta\hat{H}_{\text{ads}}(T_{j,\text{tank}}, P_{j,\text{tank}}) + \hat{H}_{\text{H2}}(T_{j,\text{tank}}, P_{j,\text{tank}})\right] \\ & + m_{j,\text{H2,gas,tank}} \cdot \hat{H}_{\text{H2}}(T_{j,\text{tank}}, P_{j,\text{tank}}) \\ & + m_{j,\text{H2,gas}} \cdot \hat{H}_{\text{H2}}(T_{j,\text{gas}}, P_{j,\text{gas}}) \\ & + m_{\text{ads}} \cdot \hat{U}_{\text{ads}}(T_{j,\text{tank}}, P_{j,\text{tank}}) \\ & + m_{\text{wall}} \cdot \hat{U}_{\text{wall}}(T_{j,\text{tank}}, P_{j,\text{tank}}) \end{aligned} \tag{9}$$

Specific internal energy and enthalpy are both expressed in kJ/kg, the first one is equal to zero since the tank is kept at a constant temperature, while the second one was obtained using the CoolProp Python library by providing the temperature and pressure of the tank at the j-iteration as input. The term $\Delta\hat{H}_{\text{ads}}$ represents the isosteric heat of adsorption in kJ/kg and characterizes the amount of heat released or required during the adsorption/desorption process. Typically, the adsorption process involves a heat

release contributing to the increase in system temperature; while during the desorption process, supplying heat facilitates the release of molecules stored in the MOF. This term can be considered, depending on the situation, a generation or a sink term. For simplicity, the isosteric heat of adsorption was assumed constant for each material, and the isosteric heat of desorption is supposed to be equal to that of adsorption but with the opposite sign. Simultaneously, the specific enthalpy was computed for each iteration under the specific system condition, given the strong dependency on storage conditions which vary significantly. The amount of hydrogen in gaseous form outside of the tank is not accounted for as it falls outside the control volume's domain. Considering that the tank is kept at a constant temperature, the terms representing the internal energy of the adsorbent material and the vessel itself are null. Therefore, equation 9 is simplified to 10.

$$\begin{aligned} H_j = m_{\mathrm{H2,solid}} \cdot \left[\Delta \hat{H}_{\mathrm{ads}}(T_{j,\mathrm{tank}}, P_{j,\mathrm{tank}}) + \hat{H}_{\mathrm{H2}}(T_{j,\mathrm{tank}}, P_{j,\mathrm{tank}})\right] \\ + m_{j,\mathrm{H2,gas,tank}} \cdot \hat{H}_{\mathrm{H2}}(T_{j,\mathrm{tank}}, P_{j,\mathrm{tank}}) \end{aligned} \tag{10}$$

2.1.2 Heat Losses

Within the scope of this study, the analysis centered exclusively on convective heat losses occurring between the tank and the external environment. This focus stemmed from the hypothesis that radiative and conductive losses, particularly those between the tank and its supporting structure, are negligible in the context of this model.

$$Q_{\mathrm{loss}} = h \cdot A_{\mathrm{tot}} \cdot (T_{\mathrm{storage}} - T_{\mathrm{amb}}) \tag{11}$$

$$h = \frac{1}{\left(\frac{\ln(r_{tank,o}/r_{tank,i})}{2\pi k_{tank} L_{tank}} + \frac{\ln(r_{ins,o}/r_{ins,i})}{2\pi k_{ins} L_{ins}}\right)} \tag{12}$$

Heat losses are significantly affected by both the geometry and material composition of the tank, emphasizing the importance of careful consideration when selecting tank technology. Hydrogen tanks are categorized into five different types based on the purpose, pressure, and material of the vessel. Type 3 and 4 are the most advanced technologies. These two types of tanks are commonly used for hydrogen storage in cars, mainly due to their lighter weight compared to other types available. In this case study, we considered a type 3 tank, specifics presented in Table 2.1.2, made of T700S Carbon Fiber with Al 2024 alloy liner and Multi-Layer Vacuum Super Insulation [33]. This tank, represented in Figure 14, consists of a liner, a metallic lining made of Al 2024 alloy, which ensures excellent mechanical properties. Immediately after there is a layer made of T700S carbon fiber, this material allows the tank to withstand higher internal pressures while having a lower overall weight. Following this, there is a vacuum layer to minimize heat exchange with the surroundings, and finally, an outer shell made of Al 2024 alloy. In this tank, hydrogen can be compressed to a higher pressure, thus enabling the transportation of a larger quantity of gas in a smaller tank.

Tank Parameter	**Value**	**Unit**
Volume	50	L
Mass	63	kg
Diameter	0.227	m
Height	1.680	m
Effective conductivity insulation layer	$5.2 \cdot 10^{-4}$ [33]	W/mK
Thickness of the tank	0.05	m
Thickness of the insulation layer	0.05	m
Specific heat tank ($c_{p_{tank}}$)	0.752 [34]	J/gK
Thermal conductivity tank (k_{tank})	6.9 [34]	W/mK

Table 3: Tank characteristics.

One crucial parameter is the total volume of the storage, which is calculated during the simulation and depends on the specific case study, in this case, it is determined by the maximum energy capacity of the storage and the maximum pressure inside the tank. From an engineering point of view, using multiple smaller tanks, such as a bundle of cylinders, is preferable to using a larger tank if a greater volume is required. This simplifies the modeling process, as the total storage volume can be divided by the volume of each cylinder to determine the number of cylinders needed to store the required amount of hydrogen.

Consequently, when calculating heat losses due to convection, it will be necessary to multiply the number of cylinders by equation 11.

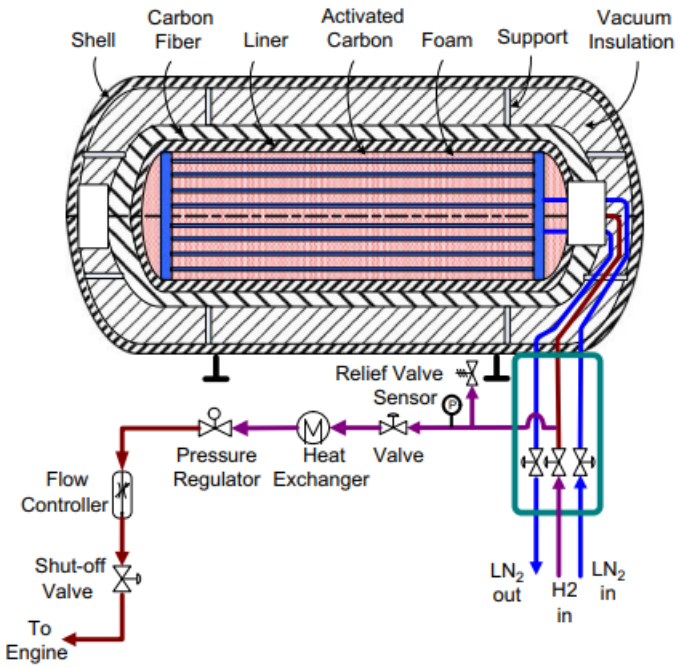

Figure 14: Type 3 tank layout [33].

2.1.3 Cooling System

This chapter outlines the primary role of cooling in enhancing hydrogen adsorption, detailing the operational phases, technology choices, and the development of a practical model to simulate and evaluate cooling strategies.

To optimize hydrogen storage in adsorbent materials, it is essential to operate at lower temperatures, as these conditions enhance the adsorption process. The process of hydrogen adsorption by a solid is characterized by the uptake of the gas molecules in the volume of the adsorbent, where the attractive forces of the solid surface are strongest. The total amount of molecules in this defined area is also known as absolute adsorption. On the other hand, the measured quantity, also known as excess absorp-

tion, is calculated relative to a system that does not adsorb gas. The excess adsorbed amount thus indicates the portion of molecules within the adsorbent's volume attributed to the interactions between the solid and gas [35]. Hydrogen adsorption in various nanostructured adsorbents, including MOFs and activated carbons, has been effectively described by the Dubinin–Astakhov micropore filling model, expressed in 13. These materials demonstrate significant hydrogen uptake at low temperatures, close to 77 K and their hydrogen adsorption capacity sharply decreases as the temperature rises. The decrease in adsorption capacity with increasing temperature is coupled with a shift in the isotherms towards a more linear regime, highlighting a change in the adsorption behavior (Figure 15). The enhanced adsorption efficiency at lower temperatures is attributed to the more effective capturing of molecules with lower thermal energies by the surface's attractive potential [35].

$$n_{tot} = n_{max} \cdot \exp\left[-\left(\frac{RT}{\alpha} + \beta T\right) \ln^2 \frac{P_0}{P}\right] \tilde{\rho}_{H_2} \left(\frac{1}{\rho_{bulk}} - \frac{1}{\rho_{He}}\right) \tag{13}$$

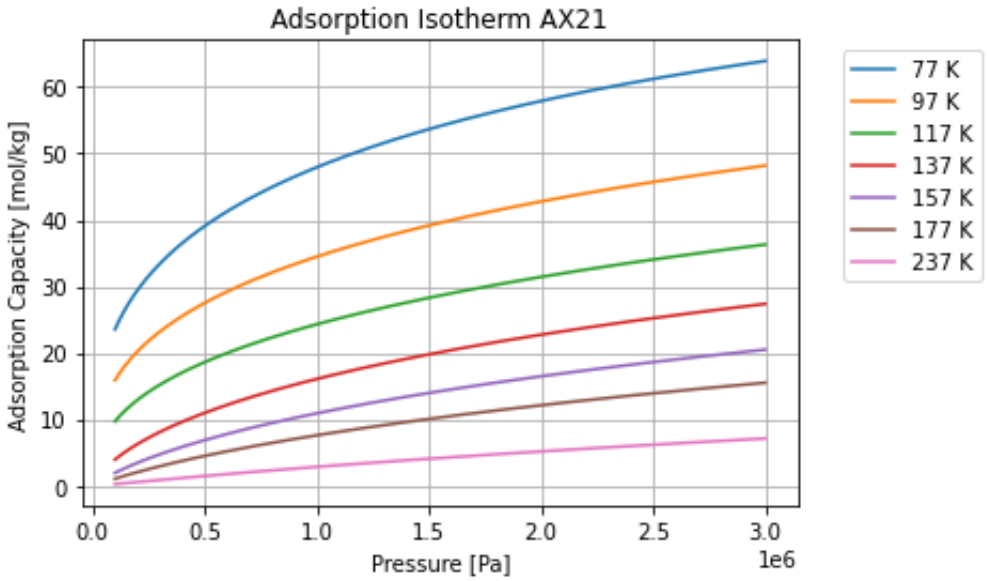

Figure 15: AX21 and H_2 adsorption isotherms at different temperatures. Data fitting based on the results reported by [36].

Due to the mentioned reasons, it is therefore clear that advanced cooling techniques are necessary in the context of hydrogen storage by physisorption, particularly when it comes to the management of storage vessels. In this case study, the cooling process begins with the precooling of incoming hydrogen to a temperature of 25 °C, using a simple technology such as a water cycle, this initial cooling step is crucial for preparing the hydrogen for further temperature reduction. As hydrogen transitions from ambient to close to cryogenic temperatures (down to 77 K), more complex cooling technologies are required. Among these, the Joule-Thomson (J-T) cooling cycle, or Linde cycle, stands out for its simplicity and efficiency (Figure 16). This recuperative cycle is particularly suitable for high-pressure operations, offering a simple layout and good scalability, albeit with a higher energy cost. Alternative regenerative cycles, while more energy-efficient,

suffer from complexity, higher costs, and scalability issues. Given the thesis's focus on simulating several scenarios, a simple and scalable cooling cycle like the J-T cycle is preferred.

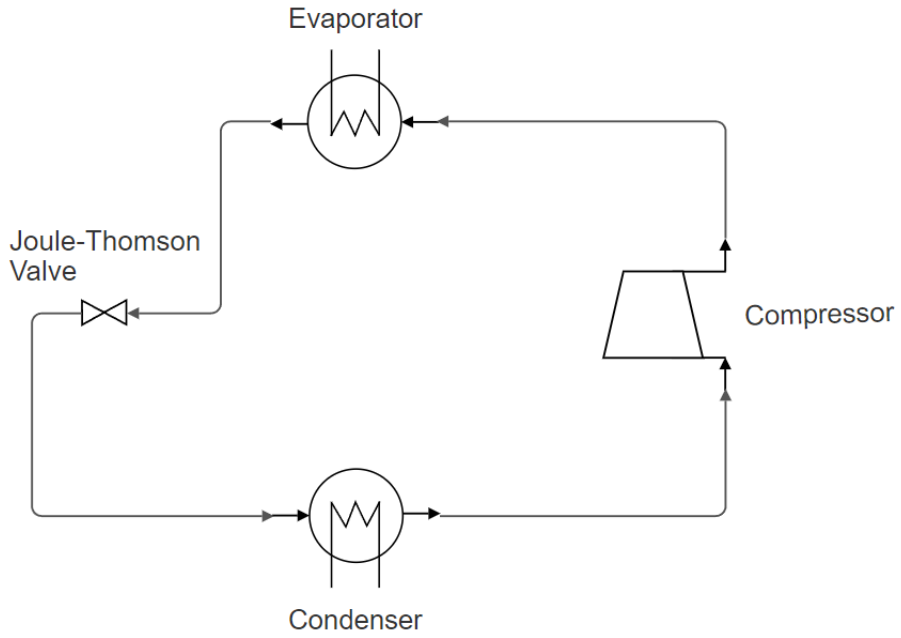

Figure 16: Joule-Thomson cycle.

The effectiveness of the Joule-Thomson cycle lies in its simplicity, consisting of a condenser, compressor, evaporator, and Joule-Thomson valve. The choice of refrigerant and the need for different precooling stages depend on the target temperatures. For precooling, cascade cycles using different refrigerants can efficiently lower the coolant to the desired temperature.

A model for each cooling cycle was developed using Aspen Hysys, a process simulation software, with working points reported in the literature [37]. The integration of Python with Aspen Hysys facilitated the direct communication of essential parameters, such as the evaporator's duty ($Q_{c/h}$), to

the simulation. By providing as input the evaporator duty, the simulation returns valuable system operation data, including pressure, temperature, mass flow rate, and what is most interesting and useful in this case, compressor power. This data enables accurate calculation of the energy costs associated with cooling the system to the desired temperature.

In these refrigeration processes, a value of 5°C has been selected as the temperature difference driving heat transfer in the evaporator heat exchanger, which is economically optimal for low-temperature processes [37]. Therefore, the refrigerant in the cooling cycle, at the inlet of the evaporator, will be 5°C lower than the desired temperature for the cooling process. As previously mentioned, various refrigerants can achieve different temperatures. For the specific case of the single-stage cooling process at -25°C, different liquids can be employed as shown in Figure 17. Ammonia was selected due to its lower compression power requirement to achieve comparable results compared to using propylene in the single-stage setup. However, to achieve lower temperatures such as -50°C, ammonia was no longer suitable. Using a single stage and propylene as refrigerant, made it possible to reach the desired temperature (Figure 18).

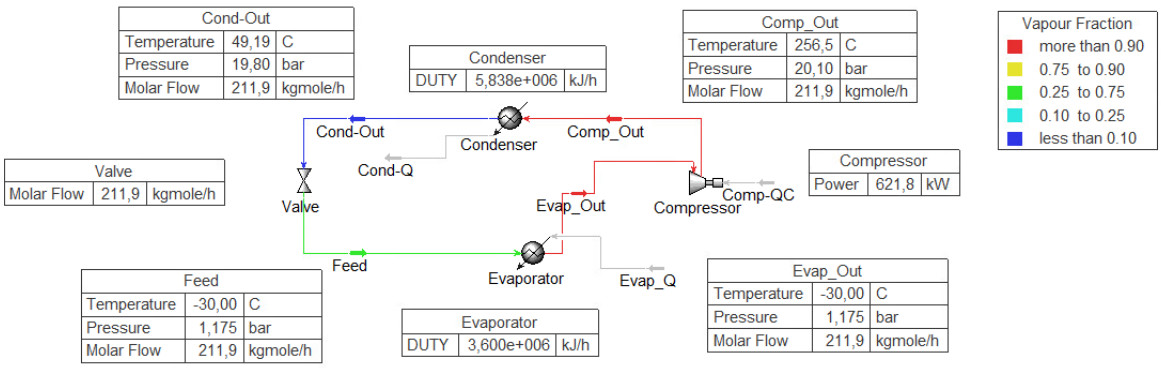

Figure 17: Ammonia single stage at -30°C in Aspen Hysys for -25°C cooling process.

.

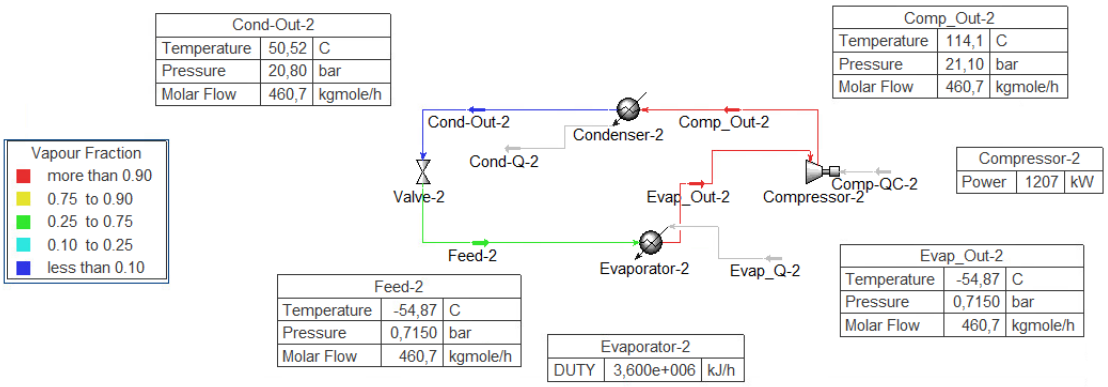

Figure 18: Propylene single stage at -55°C in Aspen Hysys for -50°C cooling process.

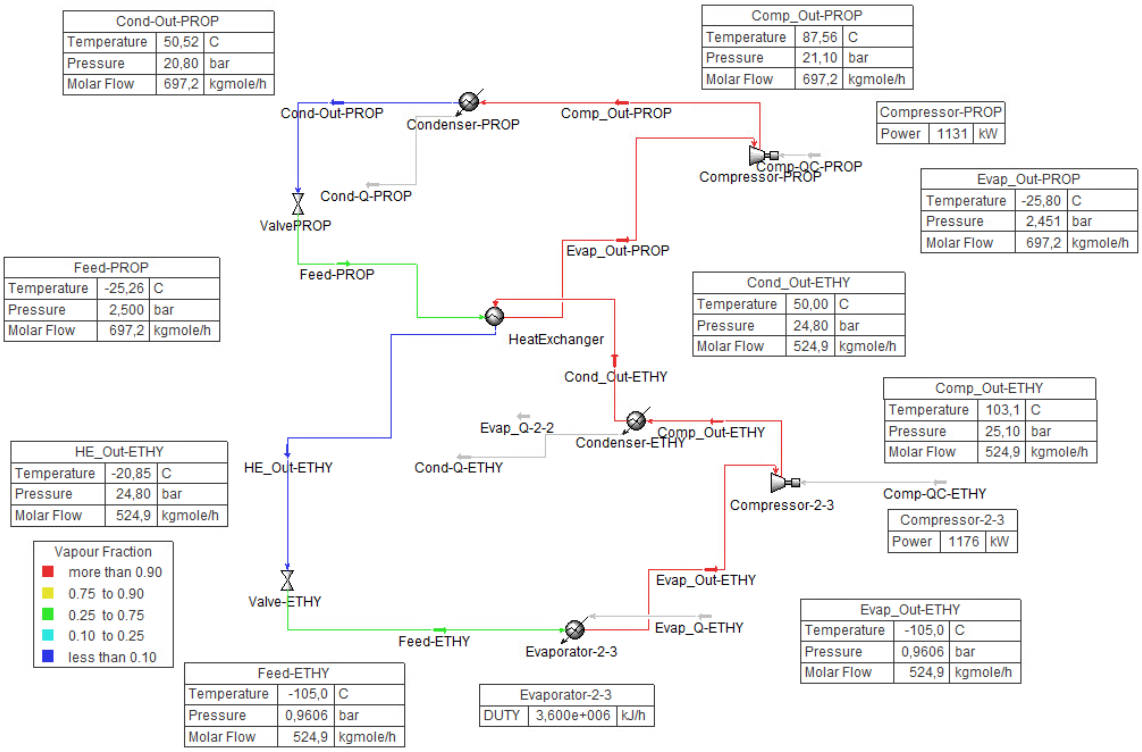

Figure 19: Ethylene-Propylene two stage at -105°C in Aspen Hysys for -100°C cooling process.

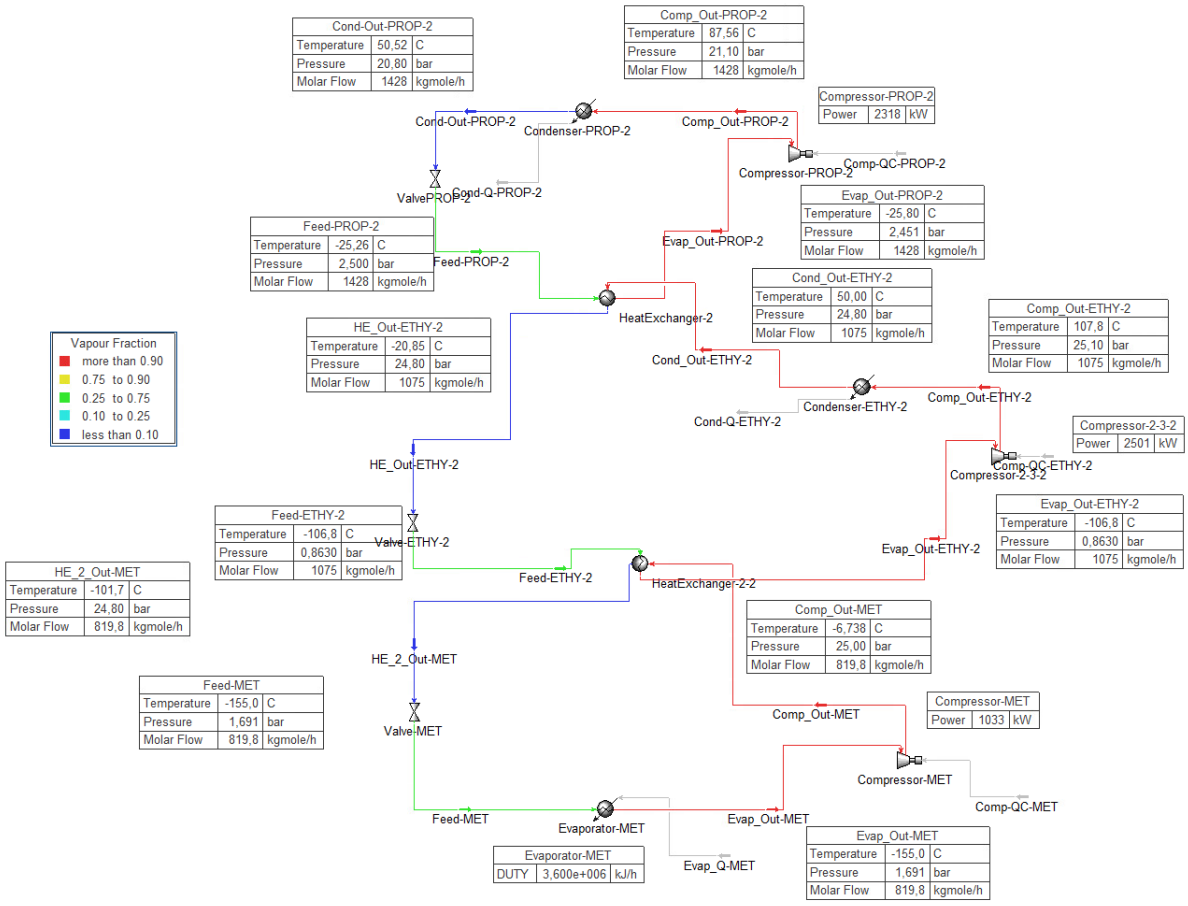

Figure 20: Methane-Ethylene-Propylene two stage at -155°C in Aspen Hysys for -150°C cooling process.

To achieve extremely low temperatures, it is necessary to use nitrogen (21), cooled to low temperatures through cascade cycles. If even lower temperatures are desired, simply adding additional stages using suitable refrigerants would be necessary, a list is presented in Figure 22, albeit increasing the costs of the system and compressor consumption.

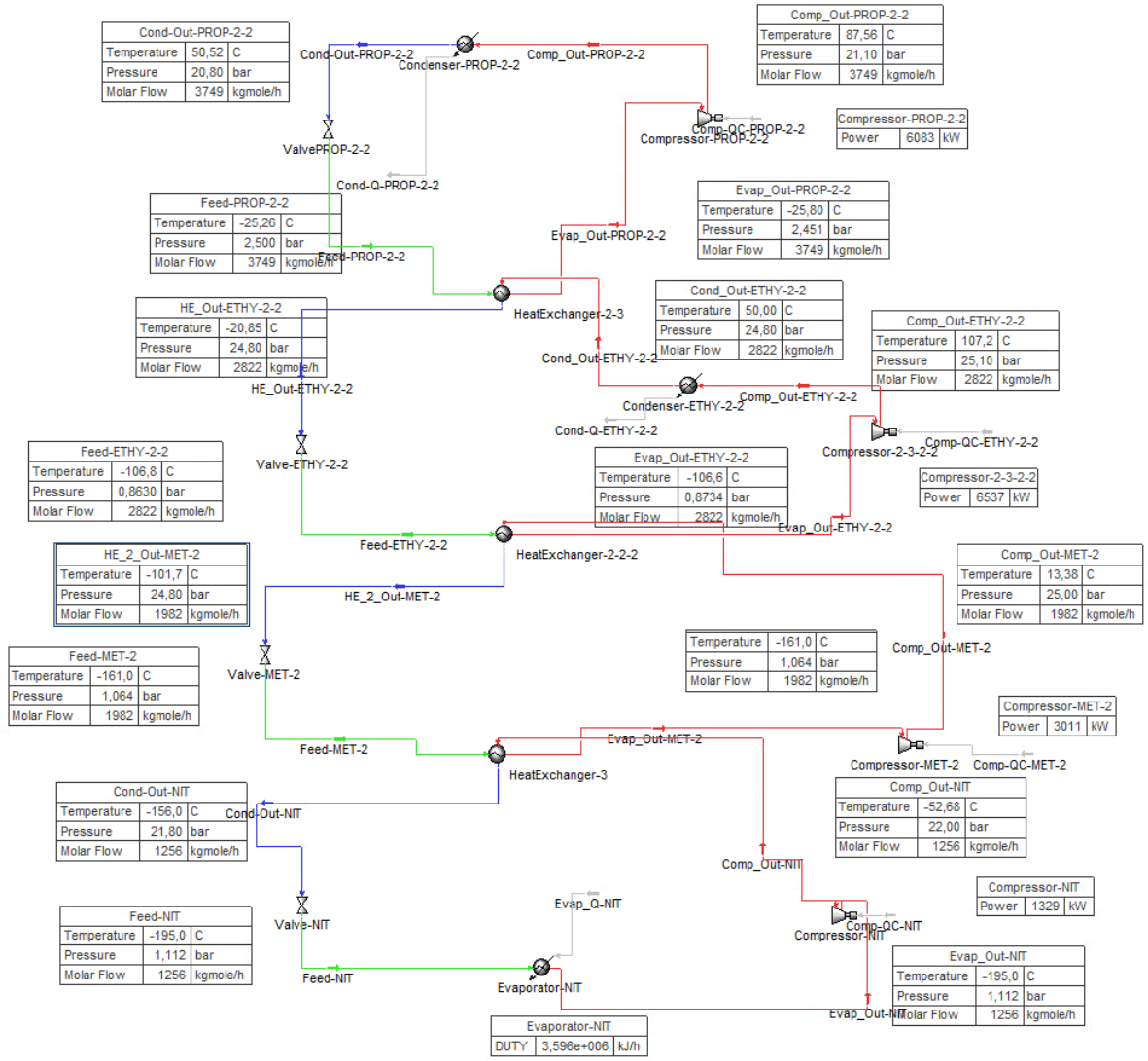

Figure 21: Nitrogen-Methane-Ethylene-Propylene two stage at -195°C in Aspen Hysys for -190°C cooling process.

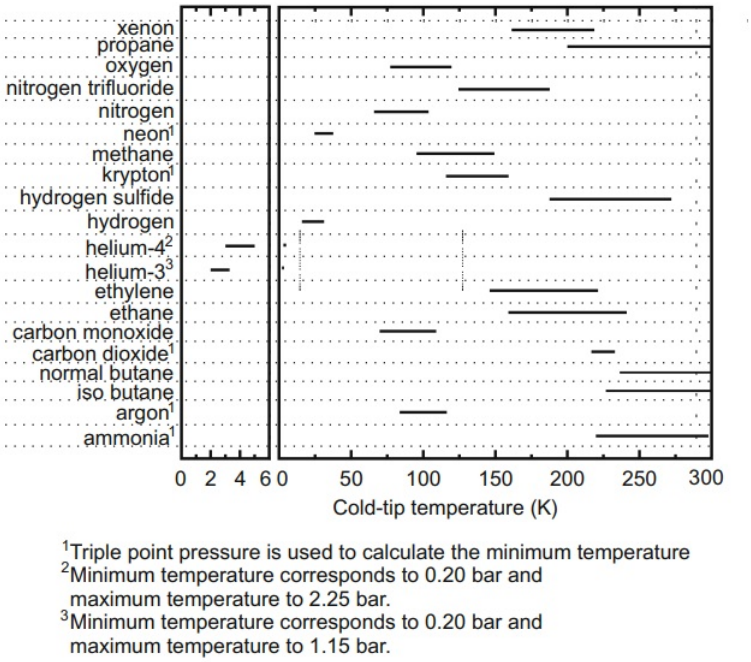

Figure 22: JT cooling cycle fluids based on desired temperature ranges [38].

Furthermore, a compressor work map was created to guide future applications. The map presented in Figure 23, is generated through simulations across a temperature range from 273K to 83K and varying evaporator duties from 1 kW to 1 MW, provides a comprehensive overview of compressor performance at different powers and temperatures. Through double interpolation of temperature and evaporator power, the compressor's power output, and thereby the energy cost, can be precisely determined.

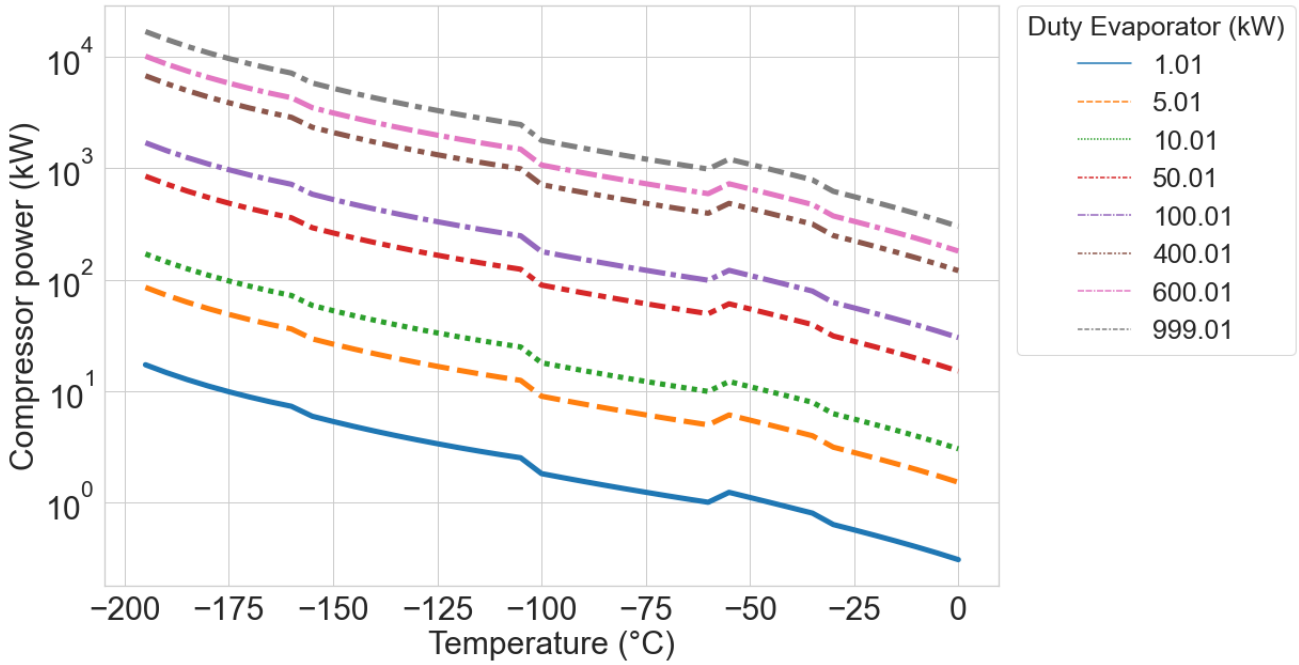

Figure 23: Compressor power map.

2.1.4 Heating System

Similar to the approach taken with the cooling system, the design, and implementation of a heating system were deemed essential to promote the release of hydrogen from the tank. This necessity arises from the exothermic nature of the hydrogen desorption process. To maintain the tank at its optimal working temperature, it becomes obvious the need to supply additional heat during the discharge phase. To address this requirement, a very simple but effective technology was chosen for its ability to efficiently provide the necessary heat. This technology is a heating wire that carries an electric current, generating heat through the Joule effect. The efficiency of the electricity-to-heat conversion process was chosen to be 95% ensuring

that the majority of the electrical energy input is effectively transformed into heat, optimizing the performance of the heating system for the hydrogen desorption process.

Both the heating and cooling systems are treated as ideal systems, meaning they are modeled with the assumption of perfect efficiency and no thermal losses between the control volume and the cooling and heating system. In this simplified setup, the heating and cooling blocks are linked to the tank through a heat exchanger. This heat exchanger ensures the balance of the heat removed from or supplied to the tank by the cooling and heating systems. In practical terms, this implies that the heat removed from the tank during the cooling phase is equal to the heat removed from the cascade cooling system by the heat exchanger. Since this is a simplification of the system, it represents a less conservative approach. Further investigation will be necessary to better design the system, taking into account the losses involved the the connection between the tank and the cooling/heating facility.

2.2 Hybrid Storage Simulation

The proposed proof of concept involves simulating a storage system utilizing a double tank configuration: in one tank occurs physisorption, while in the other chemisorption. This preliminary study aims to determine the feasibility and potential benefits of this configuration for further investigation. The focus lies in assessing whether there is an enhancement in storage capacity in real-world scenarios, considering actual production curves and load demands. A comparison between chemisorption-only storage and a hybrid system is conducted to evaluate whether the hybrid solution improves overall system capacity.

The two-tank model exploits the unique characteristics and storage capacities of the two storage systems. The physisorption tank serves as a short-term storage solution since it accounts for rapid charging and discharging processes needed to meet immediate energy demands. On the other hand, the chemisorption tank is designed for long-term storage, which can retain larger amounts of hydrogen for prolonged periods, considering the drawback of slower charging and discharging rates.

By incorporating these distinct dynamics into the model, it becomes possible to simulate and analyze the behavior of the combined short-term and long-term storage mechanisms.

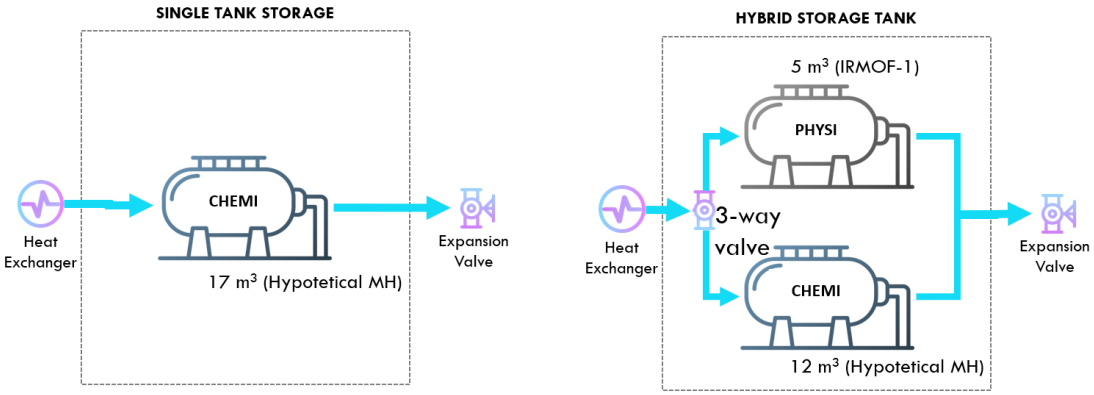

Figure 24: Hybrid storage configuration.

2.2.1 Charge Phase

During periods of electricity overproduction, the quantity of produced hydrogen is calculated and stored in the tanks. An algorithm is used to determine the optimal amount of hydrogen to store based on the available tank capacity and electricity production patterns. The charging process follows a sequential approach for filling the physisorption tank and the chemisorption tank, adhering to specific criteria (Figure 25). Firstly, the physisorption tank is filled up to 80% of its maximum capacity. When the physisorption tank reaches its designated threshold, the chemisorption tank is filled to its maximum capacity. Once the chemisorption tank reaches its full capacity, any additional hydrogen produced is directed to fill the physisorption tank up to 100%. This logic aims to ensure that in case of immediate power demand, the physisorption tank can provide energy promptly.

It's important to note that if one tank reaches full capacity during the charging process, the loading process continues exclusively in the other tank. When considering the chemisorption tank, factors such as maximum storage capacity and the maximum adsorbable molar flow rate are taken into account to ensure optimal filling conditions.

In cases where the molar flow rate from the electrolyzer exceeds the maximum adsorbable rate of the chemisorption tank, a specific protocol is followed. An amount of moles equal to the tank's maximum adsorbable quantity is adsorbed in the chemisorption tank by the metal hydrides, while any remaining moles are directed to the physisorption tank if it's not already fully loaded.

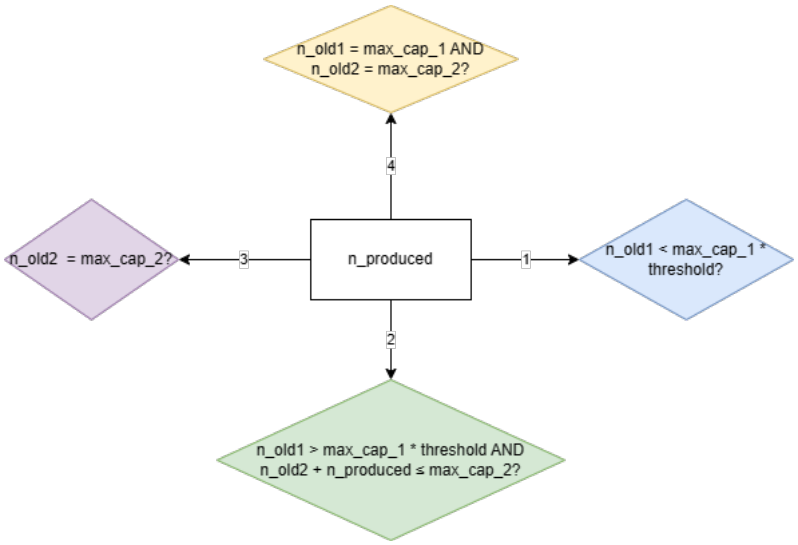

Figure 25: A potential case scenario, sequence of checks.

In Tank 1, where physisorption occurs, and Tank 2, where chemisorption takes place, the variables are defined as follows:

- n_{old} represents the quantity of stored hydrogen in the tank before the

current time step.

- n_{new} represents the quantity of hydrogen stored in the tank after adding the moles produced by the electrolyzer in this time step.
- max_{cap} refers to the maximum storage capacity of the tank, beyond which no more hydrogen can be stored.
- n_{tank} denotes the moles actually stored in the tank, corresponding to n_{EC}.
- n_{remain} represents the moles that cannot be stored in one tank and need to be checked if they can be stored in the other tank.

If it is not possible to store all the moles produced by the electrolyzer, the feasible amount of stored moles is calculated. From this value, the necessary power to be supplied to the electrolyzer to produce exactly those moles is determined and saved as *power share new*. This step is taken to avoid hydrogen overproduction. The excess electricity that is not utilized by the electrolyzer is injected into the grid. Regarding chemisorption, the variables charging rate (*ads rate*), and discharging rate (*release rate*), indicate the maximum limits at which hydrogen can be adsorbed and desorbed and are expressed in 14 and 16. The relationship between the reaction rate and species concentrations is depicted by the variable m_{ads} which is derived from the rate law governing the uptake and discharge reactions of hydrogen [39].

$$m_{ads} = C_a \cdot \exp\left(-\frac{E_a}{RT}\right) \cdot \left(\frac{P}{P_{eq}}\right) \cdot \left(\rho_{ss} - \frac{mass_{H_2,tank}}{volume_{ads,tank}}\right) \left[\frac{kg}{m^3 s}\right] \tag{14}$$

$$\ln\left(\frac{P_{eq}}{P_0}\right) = \left(a - \frac{b}{T}\right) \tag{15}$$

C_a represents the charging constant and is expressed in s^{-1}; E_a is the activation energy expressed in J/mol; R is the gas constant expressed in J/molK; P is the pressure at which the hydrogen molecules enter the tank, T is the tank temperature; P_{eq} is the equilibrium pressure, corresponding to the pressure at which the absorption and desorption of hydrogen reach the dynamic equilibrium, i.e. the rate of hydrogen absorption is equal to the rate of hydrogen desorption and is calculated with equation 15. ρ_{ss} is the density of the hydride saturated state expressed in kg/m^3.

The formulation of the equilibrium pressure varies depending on the selected metal hydride, in this case a specific material was not selected since it is a proof of concept, but to obtain more accurate results it is better to preform the simulation with a real material.

As can be seen in Figure 26, Tank 1 is prioritized for charging until it reaches the defined threshold. Checks are performed on the maximum storage capacity threshold, and calculations are made to determine the amount of H_2 moles that cannot be stored in Tank 1.

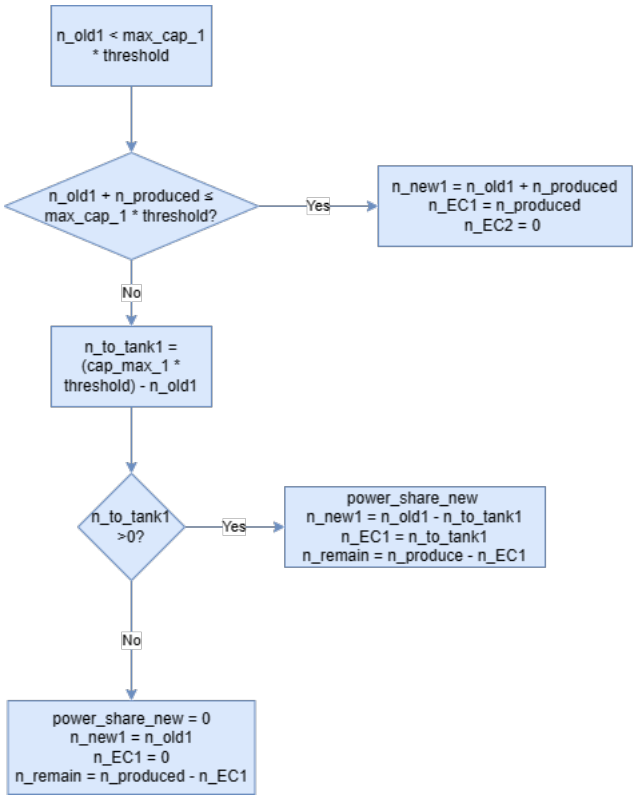

Figure 26: Charging Tank 1 until threshold.

If the hydrogen level in Tank 1 exceeds the defined threshold, a check is performed to verify if storing hydrogen in Tank 2 is feasible. It is then verified whether storing these moles would firstly exceed the maximum storage capacity of Tank 2, considering that Tank 2 must be filled to 100%, and secondly, if it would exceed the maximum charging rate (Figure 27).

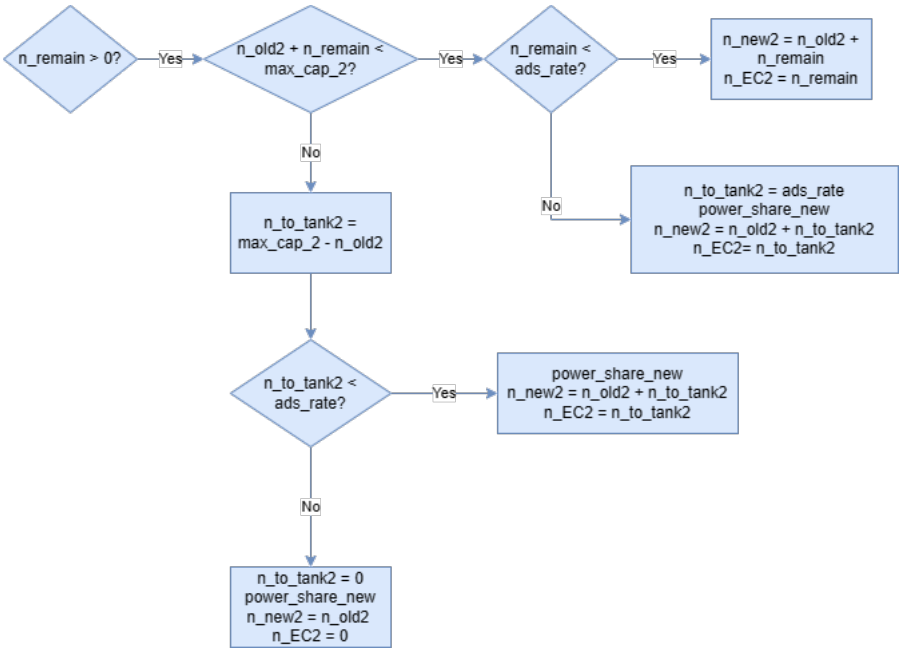

Figure 27: Surplus moles are checked for storage in Tank 2.

If, instead, the maximum filling threshold of Tank 1 is reached, and it is ensured that adding the moles produced by the electrolyzer to the moles stored in Tank 2 would not exceed the maximum capacity of Tank 2, only Tank 2 is filled. Additional checks are conducted to ensure that the charging rate for Tank 2 is not exceeded, as can be seen in picture 28.

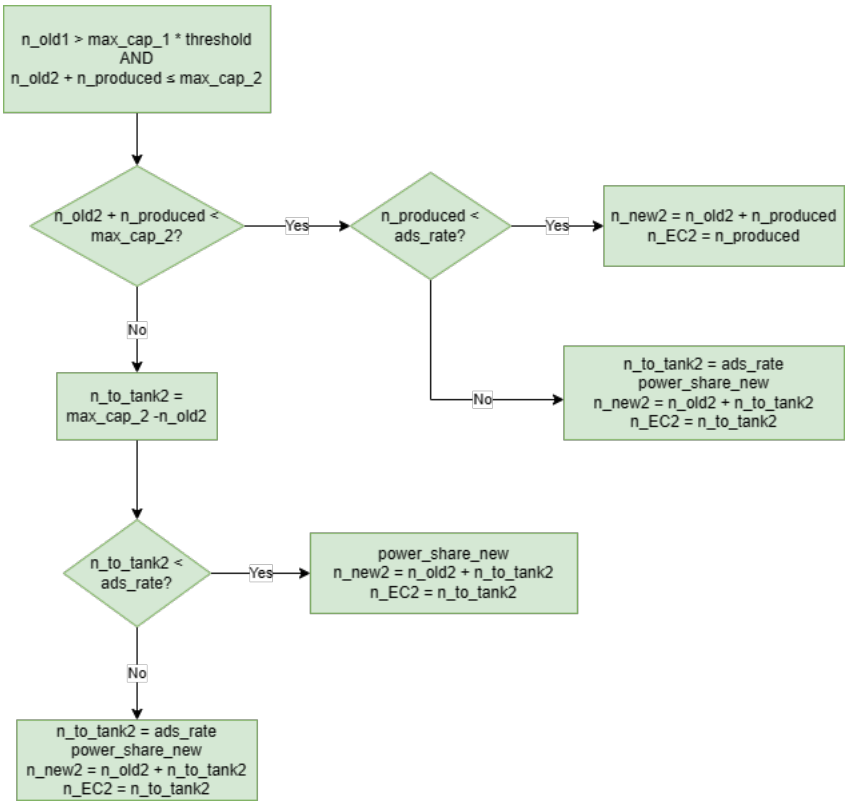

Figure 28: Charging of Tank 2.

In picture 29, it is possible to see that once Tank 2 is fully filled, Tank 1 is then filled up to 100% of its capacity.

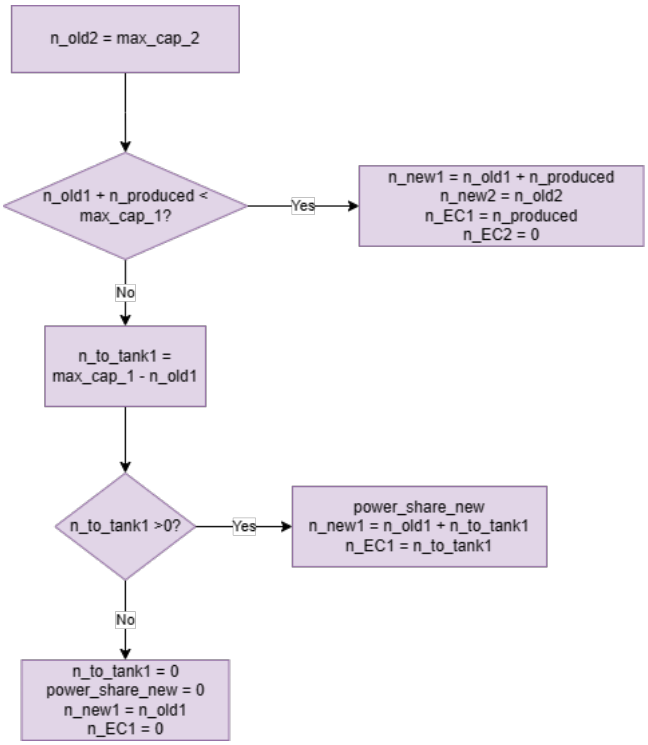

Figure 29: If Tank 2 is saturated, Tank 1 is filled up to 100%.

If both tanks are fully saturated, the entire quantity of electricity is injected into the grid, and no hydrogen production occurs (Figure 30).

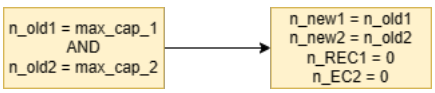

Figure 30: Tank 1 and Tank 2 are both saturated.

At the end, the sum of the moles stored in both tanks is calculated, and the power to be supplied to the electrolyzer is recalculated to ensure that only the required moles are produced.

2.2.2 Discharge Phase

When there is a demand for electricity from the load, the system calculates the amount of hydrogen required to power the fuel cell. This quantity is calculated considering the load's energy requirements and the amount of hydrogen available in the tanks. During the discharge phase, priority is given to the chemisorption tank (Tank 2), followed by the physisorption tank (Tank 1), this can be seen in Figure 31. This hierarchical approach ensures efficient utilization of stored hydrogen resources. Considerations for discharge include the maximum molar flow rate that can be released by the metal hydrides. If the required molar quantity for the fuel cell exceeds the maximum release rate from Tank 2, a specific discharge strategy is employed. An amount equal to the tank's maximum release rate is discharged from Tank 2, with any remaining moles of hydrogen discharged from Tank 1, provided it contains stored hydrogen.

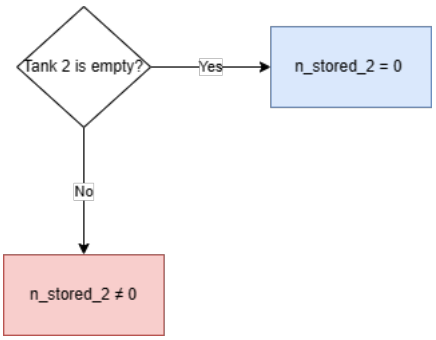

Figure 31: Check if Tank 2 is empty.

The discharge priority is assigned to Tank 2. If this tank is empty, Tank 1 is then discharged (Figure 32). The initial check verifies if it is possible to extract anything from the chemisorption tank.

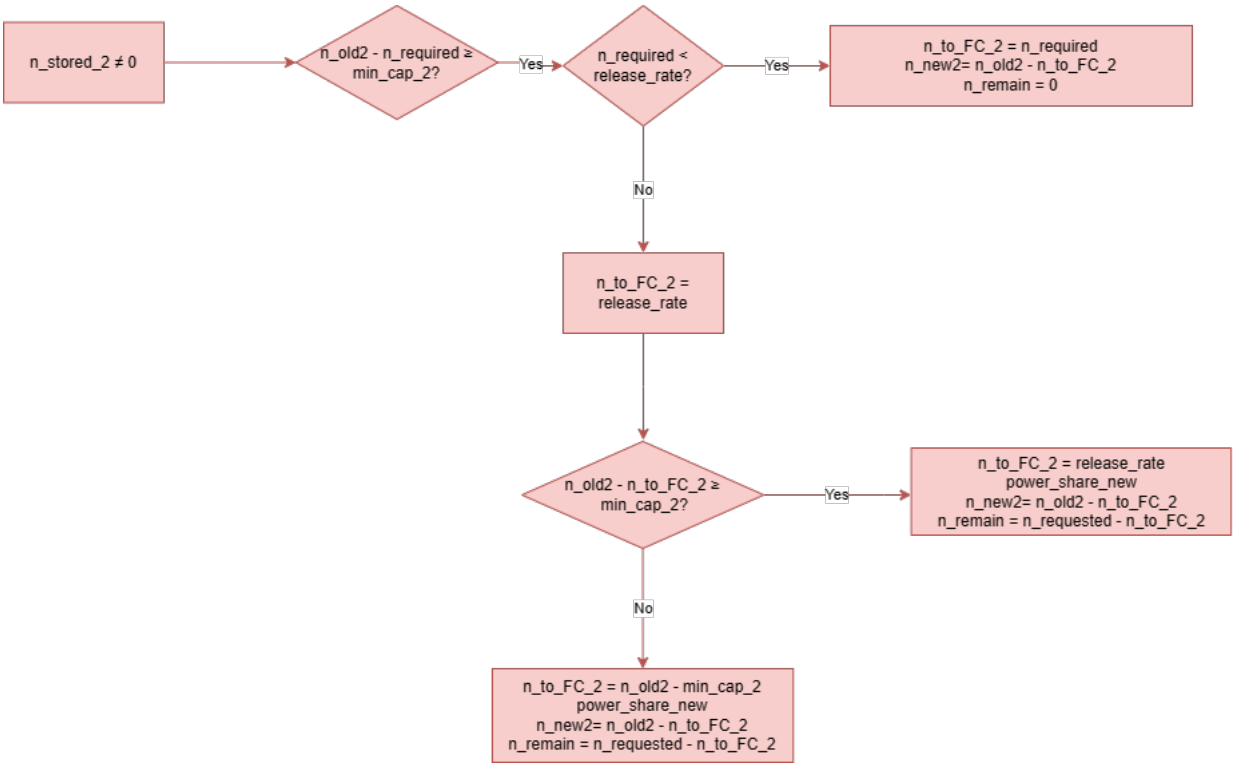

Figure 32: Tank 2 discharge logic.

The variable n_{stored_2} represents the amount of moles stored within Tank 2, $n_{required}$ is the number of moles needed by the fuel cell to meet the load demand, and min_cap_2 denotes the minimum capacity of the storage tank; the tank can not be completely emptied due to the residual moles captured within the material at 2 bar, which is the fuel cell pressure.

When after removing the required moles from the stored quantity within Tank 2, the hydrogen level in the tank still exceeds the minimum capacity of the storage, the subsequent step involves verifying whether the mole withdrawn surpasses the maximum release capacity of the tank. This denotes the limit of the chemisorption tank, which can discharge a maximum

amount of moles within a certain timeframe. Typically, the release rate is slow compared to the rapid release of physisorption.

$$m_{des} = C_d \cdot \exp\left(-\frac{E_d}{RT}\right) \cdot \left(\frac{P - P_{eq}}{P_{eq}}\right) \cdot \left(\frac{mass_{H_2,tank}}{volume_{ads,tank}} - \rho_{so,empty}\right) \left[\frac{kg}{m^3 s}\right] \quad (16)$$

C_d represents the discharging constant and is expressed in s^{-1}; E_d is the deactivation energy expressed in J/mol; R is the gas constant expressed in J/molK; P is the pressure at which the hydrogen molecules exit the tank, T is the tank temperature; P_{eq} is the equilibrium pressure calculated with equation 15. $\rho_{so,empty}$ is the density of the hydride empty state expressed in kg/m^3.

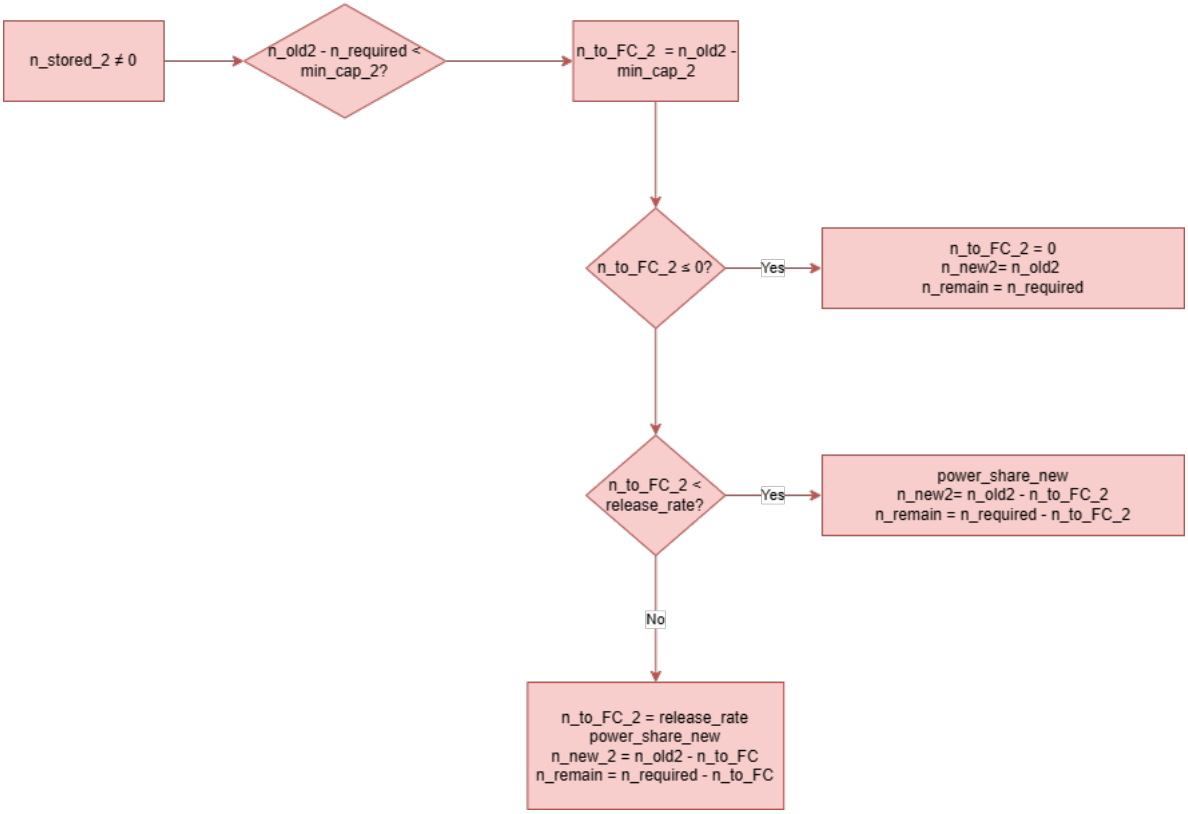

Figure 33: Tank 2 discharge logic part 2.

If, however, extracting moles from Tank 2 would result in falling below the minimum capacity, then the maximum quantity of moles that can be withdrawn from this tank is equal to the difference between the amount of moles stored at that moment and the minimum quantity of moles that can not be desorbed from the tank due to the 2 bar pressure. In this case, as well, it is checked that this quantity of moles is less than or equal to the release rate (Figure 33).

When extracting moles from Tank 2, the variable n_{remain} is calculated, which is the difference between the required moles and the moles that can

be supplied from Tank 2. This difference is useful as it allows verifying whether Tank 1 will be able to provide these moles.

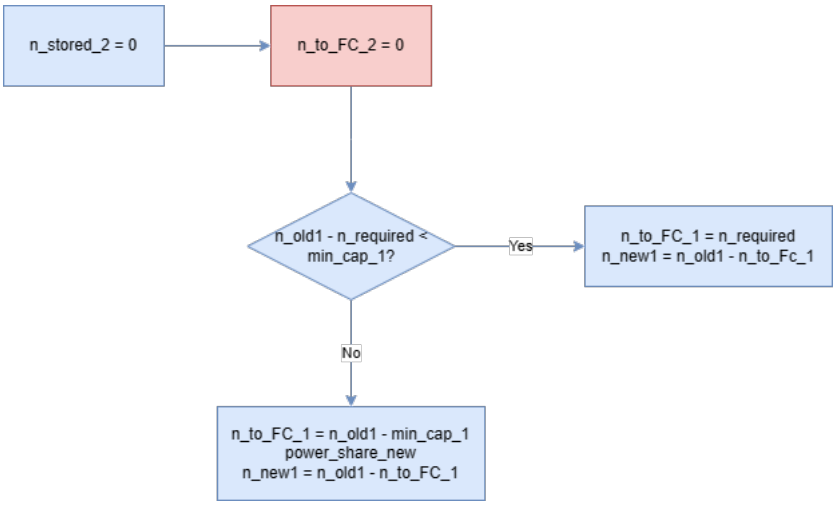

Figure 34: Tank 1 discharge logic.

If, on the other hand, Tank 2 is empty, the availability of the required moles from Tank 1 is checked, showed in picture 34. In this scenario, only the minimum capacity of Tank 1 is verified since with physisorption there is no issue concerning the mole release rate.

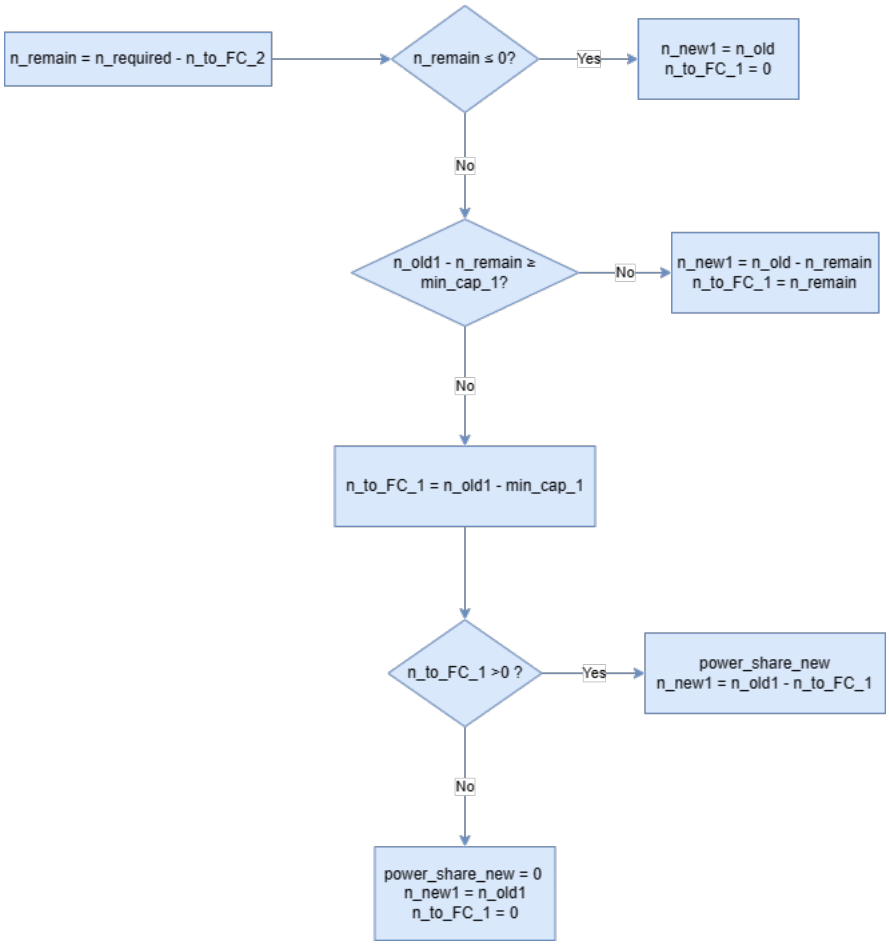

Figure 35: Tank 1 discharge logic part 2.

As previously mentioned, during the discharge of Tank 2, the presence of any remaining moles requested by the fuel cell but not supplied by Tank 2 is verified. If this quantity is greater than zero, then it is checked whether removing the required moles would still keep the system above the minimum capacity of Tank 1. If this can not be ensured, the maximum quantity of moles that allows the system to remain above the minimum capacity of Tank 1 will be withdrawn. When the storage system is unable to supply the required quantity of moles to the fuel cell to provide the adequate amount

of electrical energy required by the load, the load draws directly from the grid, extracting either entirely or partially the necessary amount of electricity (Figure 35).

3 Results

In this chapter, the results obtained from the simulations described in the methodology chapter are presented. The first section focuses on the outcomes of the thermal management of the tank, while the second section delves into the results obtained from the hybrid hydrogen storage section.

In table 4, the materials' properties are listed. It should be noted that the bulk density adopted in the simulations is the actual density reported in the literature, therefore the total volumes will be greater compared to the case where an optimized apparent density is used. Additionally, the results obtained are dependent on the materials' isotherms; changing the isotherms could lead to different results, hence the presented results might have a margin of uncertainty.

Material	Pore volume [m^3/kg]	Bulk density [kg/m^3]	Porosity [-]	Heat of adsorption [kJ/mol]
IRMOF[31]	0,005	130	0,6	-5
MSC30[31]	0,002	270	0,6	-5
AX21[40]	0,002	300	0,6	-5

Table 4: Structural properties of sorbent materials.

3.1 Thermal Management Results

The energy cost to maintain the tank at different temperatures is analyzed considering both cooling and heating, although the former contributes significantly to the overall balance. The energy cost for cooling is directly related to the use of compressors in cascade refrigeration cycles, which are employed to achieve very low temperatures. Conversely, the costs for heating were calculated based on an assumed electrical-to-thermal conversion efficiency of 0.95. As demonstrated in Section Cooling System, as temperatures decrease more compressor cycles are required to reach those temperatures. For instance, to reach 223K, only one compressor is needed, whereas to reach 77K, four compressors (from four refrigeration cycles) are required. It is evident that costs increase as temperatures decrease. Simulations were performed with maximum pressure and maximum storage capacity fixed at 30 bar and 10 MWh respectively. Consequently, the parameter derived from these boundary conditions is the tank volume. It was observed that at lower temperatures, smaller tank volumes are obtained due to the higher storage capacity of the adsorbent materials, as demonstrated by the adsorption isotherms. Figure 36 represents the energy consumption for the storage cooling and heating, and the tank volume trend as a function of the storage operating temperature. If volume is prioritized as a design parameter, it would be preferable to operate at very low temperatures. However, lower temperatures entail higher energy costs for cooling the tank and the incoming and outgoing hydrogen. A significant portion of the energy is used to cool the incoming hydrogen flow to the tank. Nevertheless, it can be seen that if volume is not a critical parameter, it would be sufficient to operate around -120°C, a temperature correspond-

ing to the current cold chain, to reduce the tank energy costs cost at the defined conditions by six times, while still maintaining a storage capacity of 10 MWh.

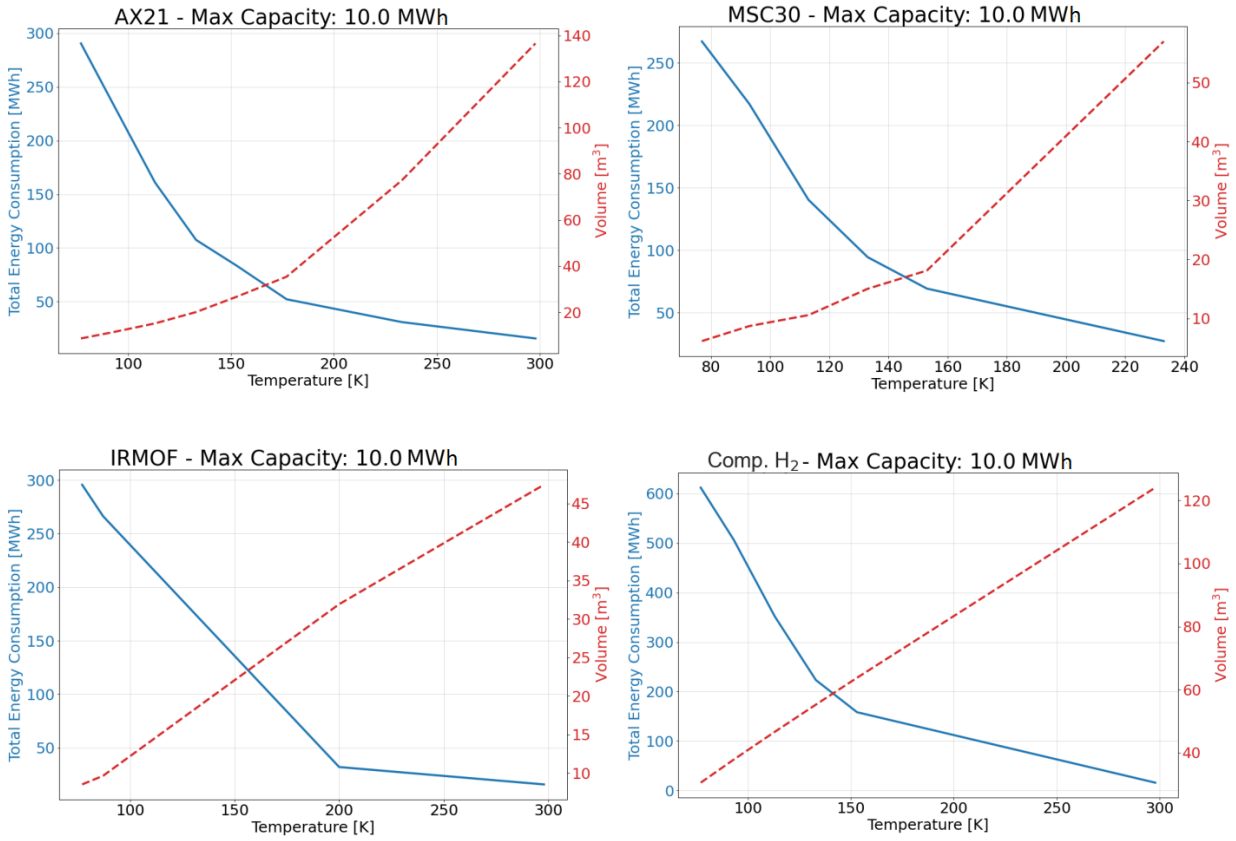

Figure 36: Comparison of energy consumption between H_2 storage by compression and physisorption.

The energy cost varies depending on the material used, but it is evident that the AX21 material outperforms others, especially when compared to an empty tank where hydrogen is compressed. Besides its low energy con-

sumption, AX21 also exhibits significantly lower volumes. It is evident that, from an energy perspective, using a material for hydrogen physisorption is advisable compared to relying solely on compression. This is likely due to the material's thermal capacity, which aids in more effective temperature control. Additionally, in the empty tank scenario, more vessels are required to store hydrogen compared to the physisorption case. The increase in total volume leads to higher losses due to convection, thereby increasing costs.

An additional consideration should be made regarding the behavior of IRMOF which exhibits energy consumption similar to that of compressed hydrogen. This is most likely because IRMOF has a very low bulk density. Indeed, the volume, in addition to being influenced by the aforementioned parameters, also depends on the bulk density. By using an optimized bulk density, it is possible to achieve more compact volumes and reduced energy consumption. In this study, the bulk densities reported in the literature from experimental results were considered. However, in Figure 37, a significant difference in the total volume can be observed between the optimized and real bulk density under the same conditions.

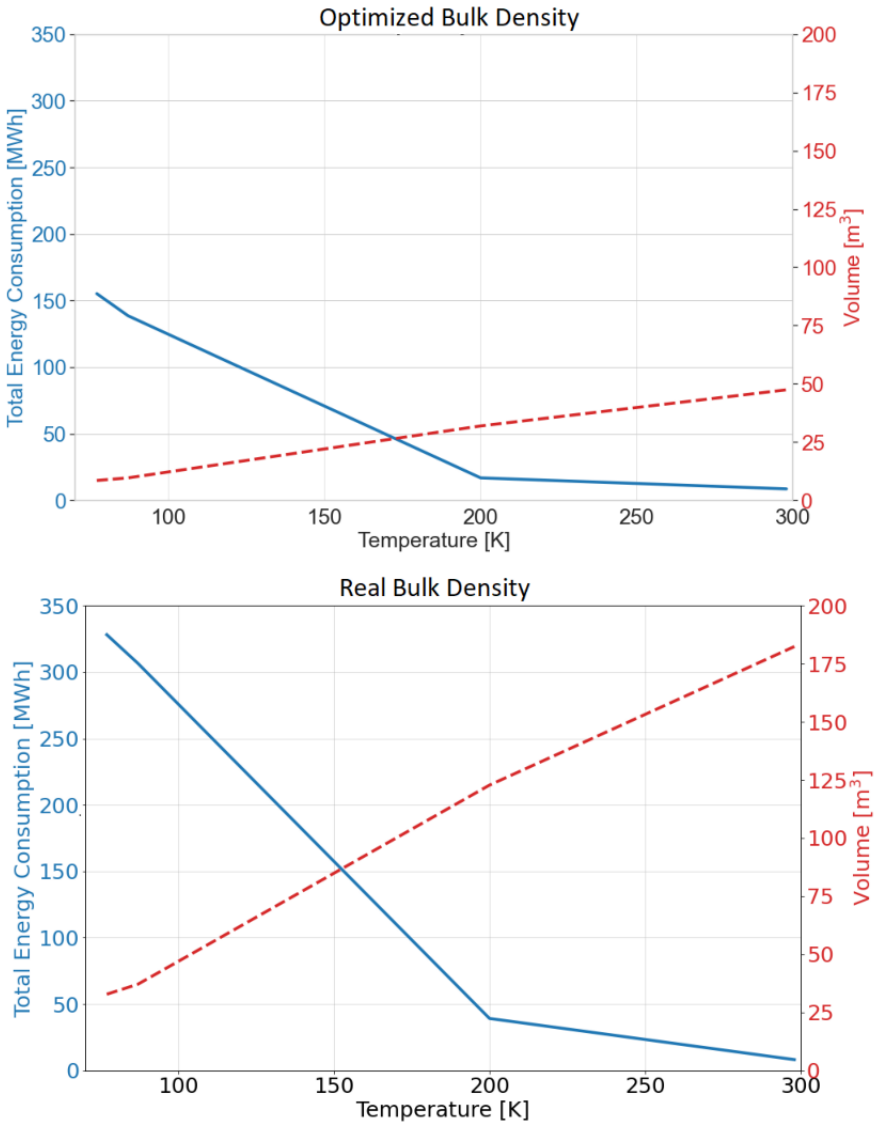

Figure 37: Volume comparison between optimal and real bulk density for IRMOF.

Other factors influencing the overall balance include the specific enthalpy, which depends on the pressure and temperature of the solid and gaseous hydrogen inside the tank, and the isosteric heat of adsorption. Fig-

ure 38 offers insights into the parameters influencing the thermal balance. The isosteric heat of adsorption is assumed constant and equal to -5 kJ/mol for all materials, as it is complex to calculate and nearly similar in the case of physisorption. This value is multiplied by the mass of hydrogen adsorbed in each timestep (Figure 38b). This parameter has a relatively limited impact compared to the contribution represented by the specific enthalpy of the stored hydrogen (Figure 38c), which is the primary contributor to the total enthalpy (Figure 38d), with a difference of two or three orders of magnitude. With a low isosteric heat of adsorption, the total enthalpy follows the trend defined by the specific enthalpy. The total power to be removed or supplied at each time step to the system (Figure 38f) is determined by the energy balance of the total enthalpy difference between the current and previous steps, heat exchange with the environment (Figure 38a), and the power to cool or heat the H_2 on entry and exit (Figure 38e). Notably the latter parameter is the primary component of the power required. Surprisingly, lower temperatures exhibit reduced convection losses, attributed to the smaller tank volumes at lower temperatures. However, it is expected that specific enthalpy is higher at elevated temperatures.

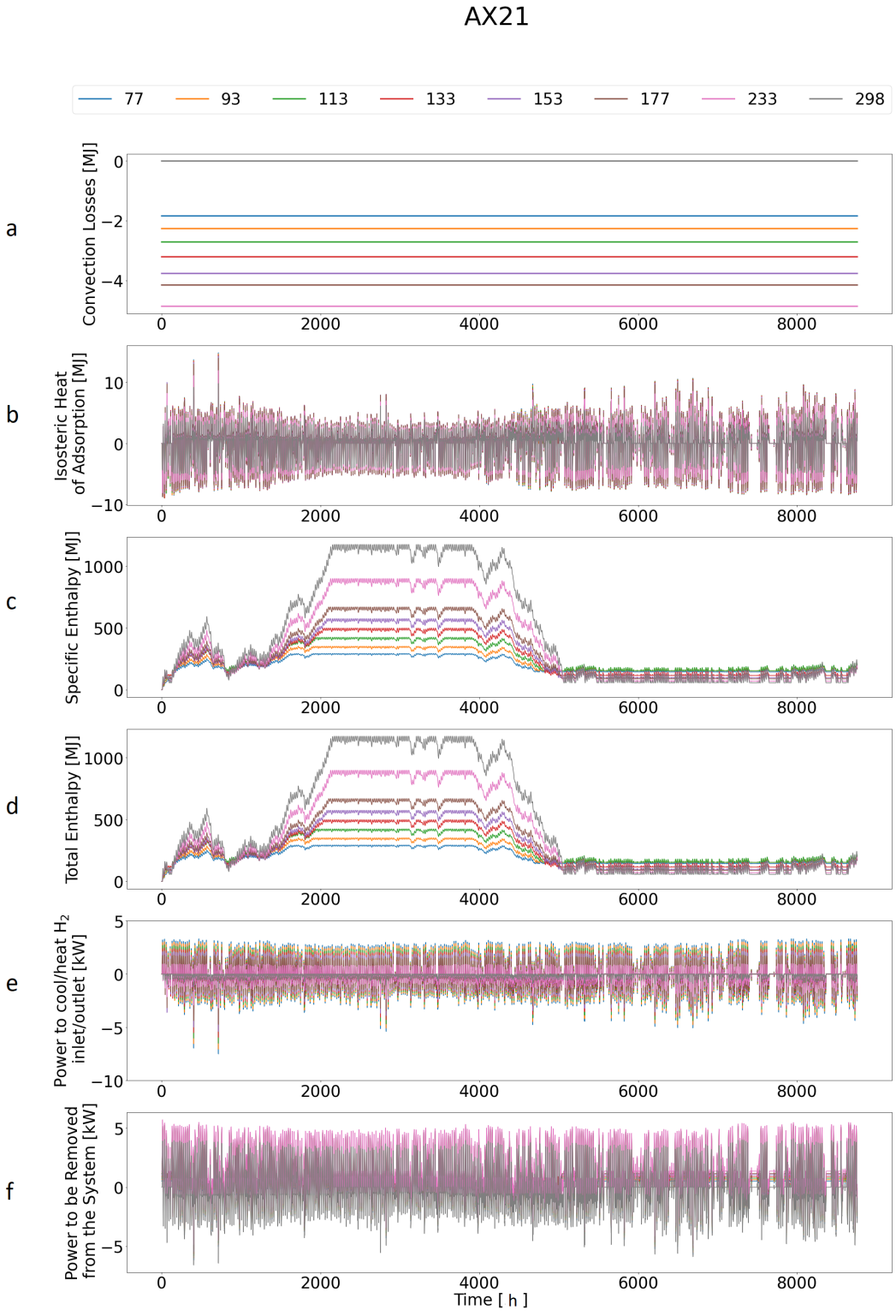

Figure 38: Parameters influencing the thermal balance of the tank filled with AX21.

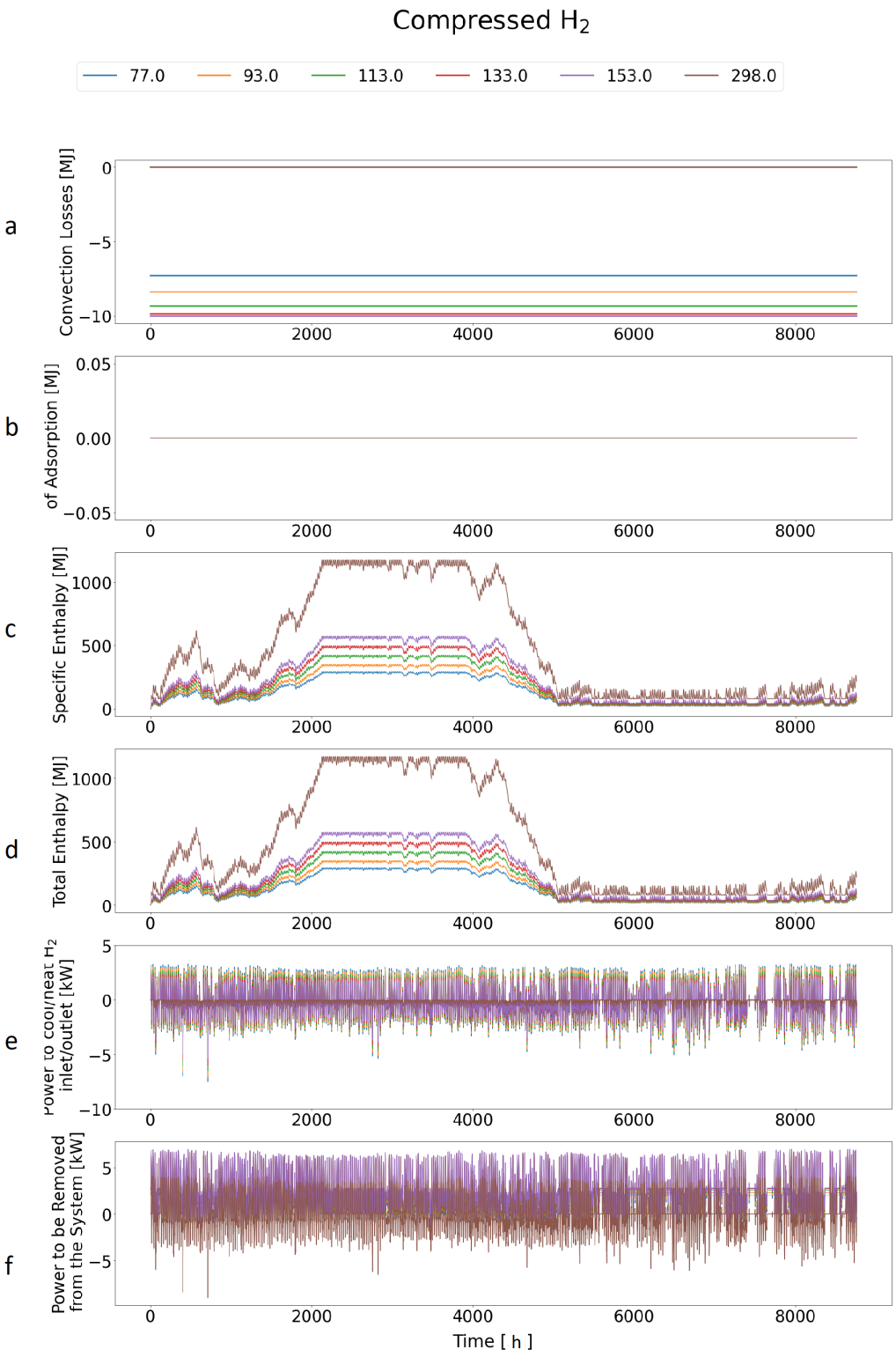

Figure 39: Parameters influencing the thermal balance of the compressed tank.

The comparison of Figure 38 and Figure 39 reveals that the losses due to heat exchange with the surrounding environment are more pronounced for compressed hydrogen storage compared to physically adsorbed hydrogen storage into the AX21 material. The absence of the term related to the heat of adsorption, although moderate, remains significant in the overall thermal balance. Indeed, refrigeration and heating systems are not employed to improve hydrogen adsorption and desorption, but only to cope with the larger losses due to heat exchange with the environment and the enthalpy of hydrogen stored in the tank. Consequently, these two factors counterbalance each other. Figure 40 compares different case studies at various temperatures and reveals that at lower temperatures, such as 77 K, IRMOF exhibits high energy costs associated with tank cooling. This can be attributed to its extremely low bulk density, leading to a large volume requirement for hydrogen storage.

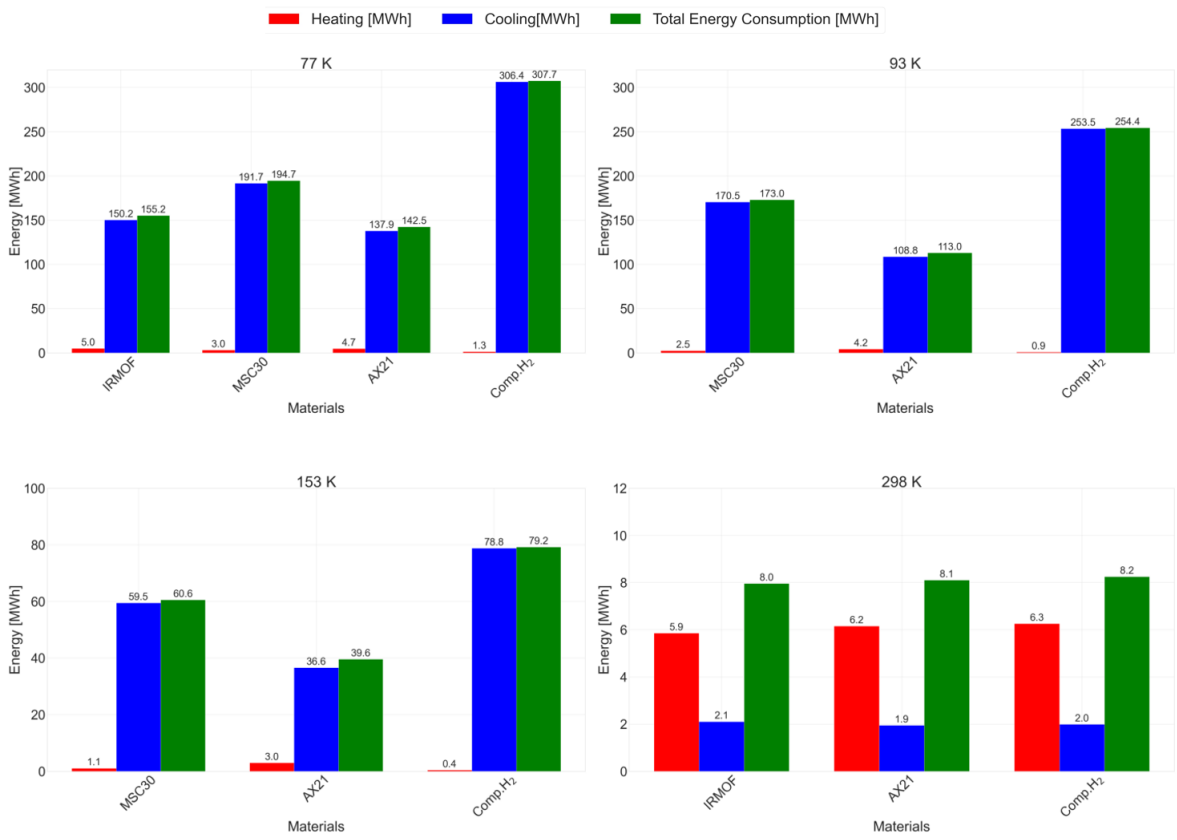

Figure 40: Total energy consumption at different temperatures and different materials.

The energy consumption of IRMOF is comparable to that of compressed-only hydrogen, again due to the large volumes needed and consequently high convection losses. In contrast, AX21 shows the best performance among the proposed cases, requiring energy expenditure half that of the compressed hydrogen case. At 93 K, the behavior is very similar to 77 K, with a slight decrease in energy consumption, but the predominant factor remains the cooling cost. The heating cost is also a factor at low tempera-

tures because the hydrogen exiting the tank needs to be heated up to the fuel cell temperature. Additionally, it may be necessary, in certain cases, to provide heat to the tank to facilitate hydrogen desorption from the material. At 153 K, there is a slight decrease in heating system consumption. This is because less heating of the outgoing hydrogen is required since the temperature difference between the hydrogen in the tank and the fuel cell is smaller compared to the cases at 77 K and 93 K. Additionally, convection losses with the environment help provide heat to the system to facilitate hydrogen desorption. The behavior at 298 K appears somewhat anomalous at first glance. Indeed, a low energy consumption related to the cooling system, required during the adsorption phase, can be observed, which was predictable. What is surprising is the increase in heating consumption. To explain this phenomenon, several considerations need to be made. Firstly, at 298 K, there are no longer losses due to convection, as this term significantly contributed to heating the tank, thus providing the necessary heat to desorb the hydrogen. Additionally, as shown in Table 5, at high temperatures, more moles of hydrogen are released overall, which will need to be heated to the operating temperature of the fuel cell. Indeed, the minimum storage capacity of the sorbent material decreases with increasing temperatures. This implies that at low temperatures, there is a greater amount of non-utilizable moles that will remain stored in the tank, as the minimum tank pressure is equal to the fuel cell operating pressure, 2 bar. In fact, from the adsorption isotherms, greater adsorption at low temperatures at the same pressure can be observed.

Temperature [K]	Capacity min [kmol]	Moles discharged [kmol]
77	67,9	4835
93	61,8	4853
113	52,4	4882
133	33,7	4937
153	24,8	4962
177	19,4	4973
233	11,3	4989
298	7,1	4997

Table 5: Minimum capacity storage for AX21 at different temperatures

Figure 41 provides a detailed overview of the annual thermal balance. The terms contributing to cooling demand include the heat exchange with the surrounding environment, the heat of adsorption multiplied by the mass of stored H_2, and the pre-cooling of incoming hydrogen into the tank. Conversely, the parameters representing the heat requirement encompass the heat demand for hydrogen desorption and for heating the hydrogen exiting the tank. During hydrogen adsorption, refrigeration cycles are employed to remove the heat released by the system, ensuring a constant tank temperature. On the other hand, during the desorption process, the convective heat exchange with the environment limits the energy expenditure. This term is regarded as a heat source within the system, enabling the balancing of the heat demand for desorption. At 298 K, convective heat exchange with the environment only occurs transiently during hydrogen adsorption. The lack of this contribution during desorption necessitates the use of a heating system to provide heat during this phase. This additional heating requirement is not present at lower temperatures, leading to increased heating consumption at 298 K compared to lower operating temperatures.

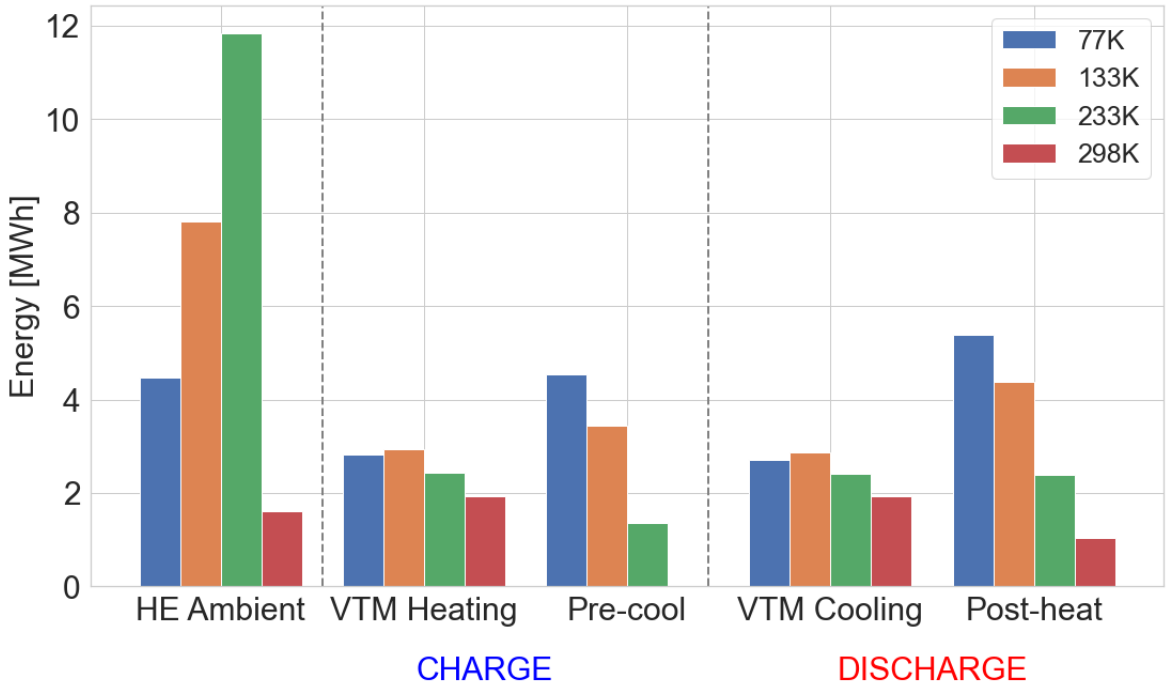

Figure 41: Thermal balance components for AX21 material at different temperatures.

Finally, Figure 42 illustrates the trend of storage efficiency trend as a function of temperature The efficiency is calculated as the ratio of useful energy output to the total energy input into the storage system, and is expressed in Equation 17. A change in the curve's slope is observable, indicating that beyond this point, increasing the temperature no longer significantly enhances the storage efficiency. Before this point, each increase in temperature corresponds to a substantial efficiency improvement. Therefore, it would be advisable to operate around the "knee" of the curve, which identifies the optimum point. Additional insights reveal that this optimum point occurs around 150K for MSC30, IRMOF and compressed hydrogen.

While for AX21, which exhibits the highest efficiency among all cases considered, the "knee" occurs at a temperature around 160K.

$$\eta_{storage} = \frac{n_{to\_FC} \times LHV_{H_2}}{(n_{from\_EC} \times LHV_{H_2}) + Energy_{cool/heat}} \tag{17}$$

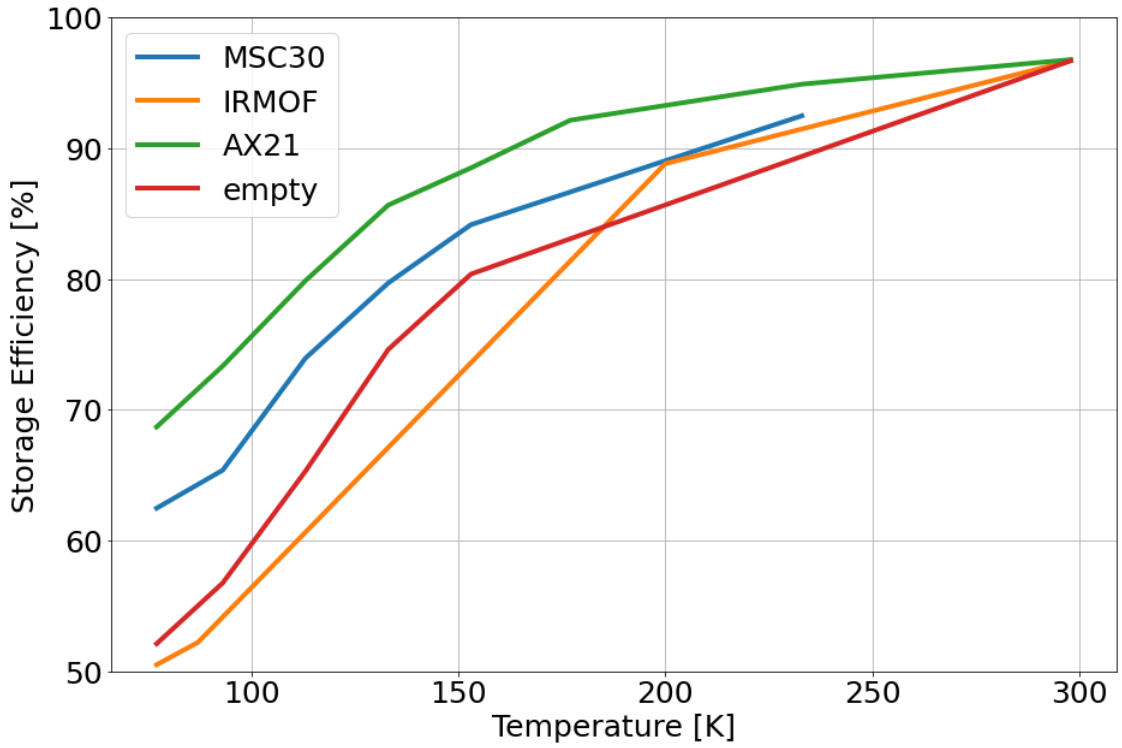

Figure 42: Storage efficiency at different temperatures.

3.2 Hybrid Storage Results

In addition to simulations on hydrogen storage via physisorption, it would be useful to investigate whether storage through chemisorption is a viable option. In this initial proof of concept, no specific material has been selected, and the rates of adsorption and desorption have been set. The purpose of this simulation is to evaluate any potential increase in storage capacity when employing a hybrid storage approach, combining chemisorption and physisorption, compared to using chemisorption alone.

Firstly, a simulation is conducted with a 17 m^3 tank containing metal hydrides, as shown in Figure 43. The tank absorbs the moles of hydrogen produced by the electrolyzer, constrained by the maximum adsorption rate. This simulation demonstrates that with this configuration, it is possible to provide the fuel cell with a quantity of moles resulting in a production of 122 MWh/year.

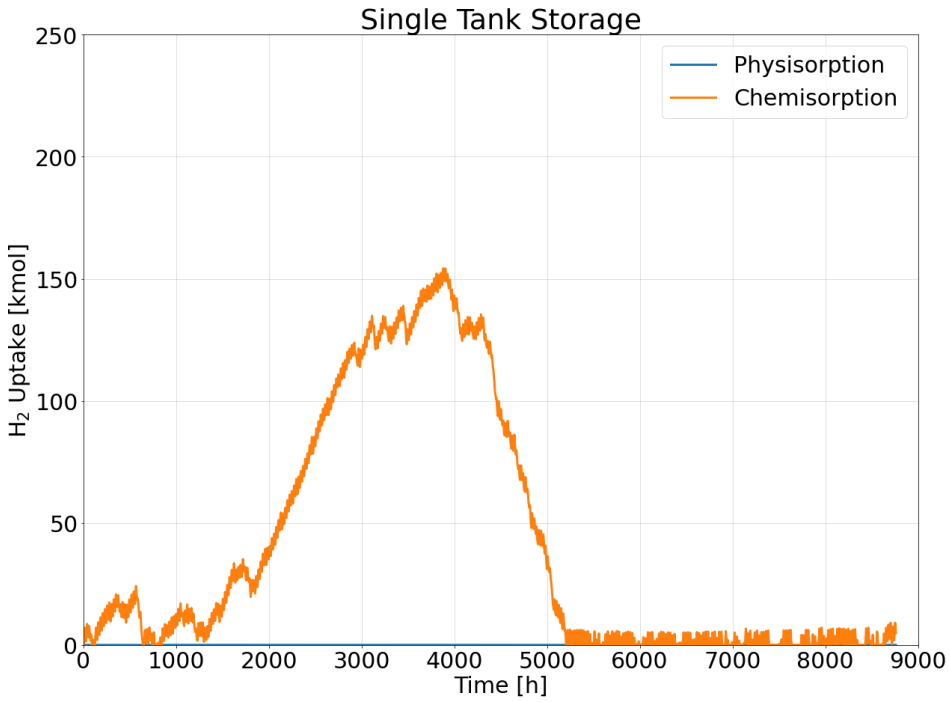

Figure 43: Single tank storage configuration.

Subsequently, while maintaining the same total volume, a second tank was introduced wherein hydrogen is physisorbed into the IRMOF material. The volume share is 12 m^3 for the chemisorption tank and 5 m^3 for the physisorption tank. Notably, only the hydrogen chemisorption process is limited by the adsorption and desorption rates, while the physisorption process does not face such constraints. As depicted in Figure 44 the total annual accumulation of hydrogen moles in the hybrid case exceeds that of the chemisorption-only setup. This is attributed to the physisorption's capability to store all the hydrogen produced by the electrolyzer and release the required moles for the fuel cell, unlike the chemisorption process. Consequently, the total energy production from the fuel cell amounts to 152 MWh/year.

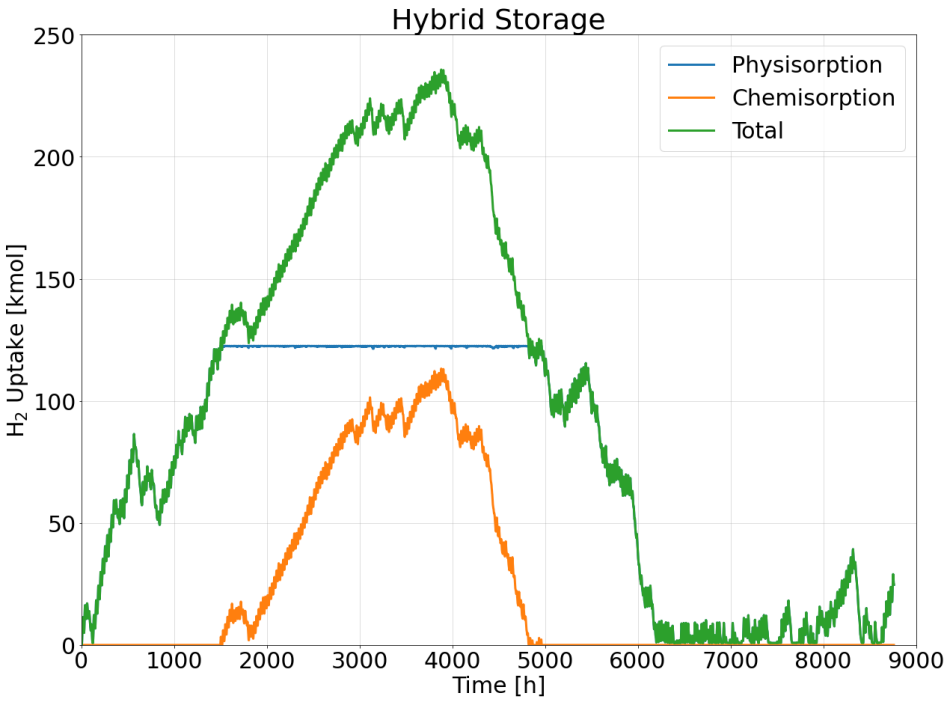

Figure 44: Hybrid storage configuration.

From Figure 45, it is evident that the hybrid solution enhances the total energy produced, bringing it closer to the load demand, thereby reducing the need to draw electricity from the grid. In fact, the hybrid storage system is capable of providing +24.8% more energy per year while maintaining the same total volume.

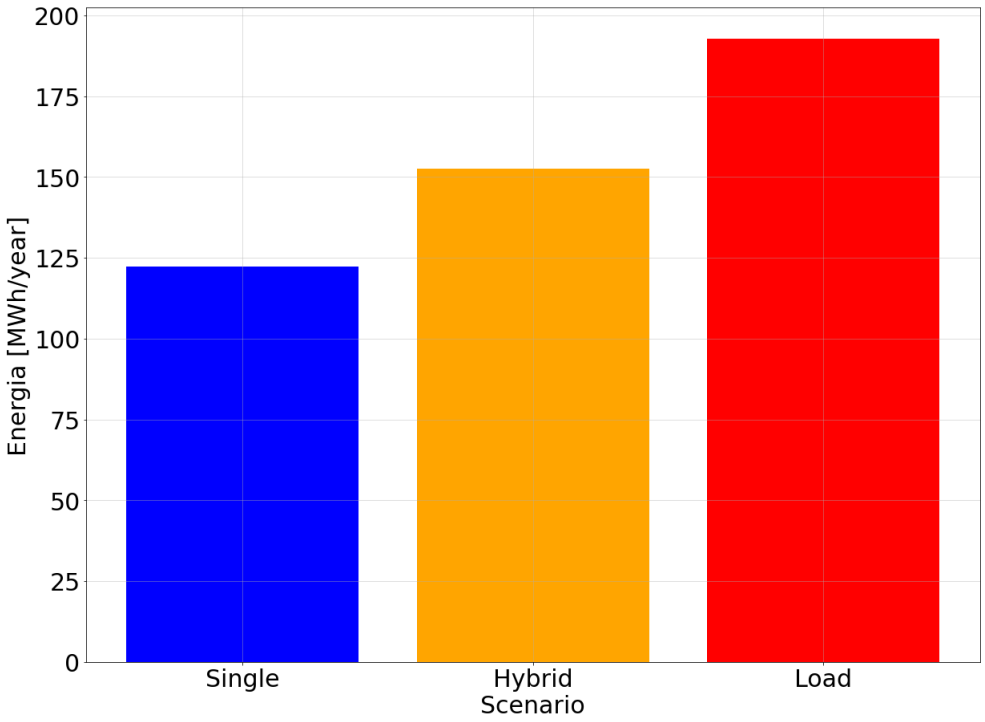

Figure 45: Single tank storage configuration.

Considering that this simulation was conducted at room temperature, further improvements could involve operating the tank where physisorption occurs at a lower temperature to enhance adsorption. Additionally, a thorough study on potential metal hydrides for storing H_2 via chemisorption would be necessary.

4 Conclusion

This thesis has provided a comprehensive analysis of thermal management and efficiency in hydrogen storage systems, with a specific focus on the outcomes derived from simulations outlined in the methodology chapter. Moreover, the thesis introduced a novel model representing the tank refrigeration system, contributing a novel approach to the existing literature.

The study on thermal management reveals significant insights into the energy consumption required to maintain the tank at desired conditions. Materials with higher bulk densities, such as AX21, demonstrate lower energy consumption and require smaller tank volumes compared to those with lower bulk densities, such as IRMOF. Furthermore, operating at lower temperatures results in reduced tank volumes but increased energy consumption due to the cooling requirements.

The analysis of storage system efficiency identifies an optimum operating temperature, emphasizing the importance of careful selection of operating temperatures to maximize efficiency. Operating around 170 K was identified as optimal, with AX21 emerging as the material with superior performance.

Additionally, the hybrid hydrogen storage section explores the potential of combining chemisorption and physisorption to increase total energy production while maintaining the same total volume. The hybrid system outperforms the chemisorption-only system, providing fuel cells with 24.8% more energy per year.

Looking forward, further improvements have been identified:

- optimize operating temperatures;

- investigate potential chemisorption materials;
- consider factors such as working pressures and system efficiency;
- focus on optimal material selection;
- develop a 3D model of the tank to accurately represent temperature distribution.

These efforts hold promise for enhancing the efficiency and effectiveness of hydrogen storage systems, which are crucial for the widespread adoption of hydrogen as a clean energy source.

References

[1] Evangelos P. Favvas. Editorial: Special issue on the membranes for carbon dioxide separation / capture applications. *Journal of Membrane and Separation Technology*, 5:1–2, 2016.

[2] Suman Karan. Environment pollution: A study on developing countries vs developed countries. *Journal of Natural Remedies*, 21:56–61, 2020.

[3] F. Pacheco Torgal. Breve análise da estratégia da união europeia (ue) para a eficiência energética do ambiente construído. *Ambiente Construído*, 13:203–212, 2013.

[4] Nguyen Van Duc Long, Le Cao Nhien, and Moonyong Lee. Advanced technologies in hydrogen revolution. *Energies*, 2023.

[5] Konstantinos Kampouris, Vasiliki Drosou, Constantine Karytsas, and Michalis Karagiorgas. Energy storage systems review and case study in the residential sector. *IOP Conference Series: Earth and Environmental Science*, 410, 2020.

[6] James E. Jr House. Chapter 7 – hydrogen. 2016.

[7] Andreas Züttel. Materials for hydrogen storage. *Materials Today*, 6(9):24–33, 2003.

[8] Peter Hoffmann and Byron L. Dorgan. Why hydrogen? the grand picture. 2012.

[9] Frano Barbir and Northpoint Pkwy. Safety issues of hydrogen in vehicles. 2012.

[10] Min Ju Chae, Ju Hyun Kim, Bryan Moon, Simon Park, and Young Soo Lee. The present condition and outlook for hydrogen-natural gas blending technology. *Korean Journal of Chemical Engineering*, 39(2):251–262, 2022.

[11] Andreas Züttel, P. Wenger, Samuel Rentsch, P. Sudan, Philippe Mauron, and Ch. Emmenegger. Libh4 a new hydrogen storage material. *Journal of Power Sources*, 118:1–7, 2003.

[12] Giuseppe Sdanghi, Gaël Maranzana, Alain Celzard, and Vanessa Fierro. Review of the current technologies and performances of hydrogen compression for stationary and automotive applications. *Renewable and Sustainable Energy Reviews*, 2019.

[13] Karpenko Im. Hydrogen: state of the art and directions of future use. *International Journal of Biosensors & Bioelectronics*, 2021.

[14] Daniela Teichmann, Wolfgang Prof. Dr. Arlt, and Peter Wasserscheid. Liquid organic hydrogen carriers as an efficient vector for the transport and storage of renewable energy. *International Journal of Hydrogen Energy*, 37:18118–18132, 2012.

[15] Gregor Erbach and Liselotte Jensen. Eu hydrogen policy - hydrogen as an energy carrier for a climate-neutral economy, 2021.

[16] Christos M. Kalamaras and A. M. Efstathiou. Hydrogen production technologies: Current state and future developments. 2013.

[17] Nafion. Membranes for fuel cells. White Paper, s.d. Accessed: March 15, 2024.

[18] Cosetta Ciliberti, Antonino Biundo, Roberto Albergo, Gennaro Agrimi, Giacobbe Braccio, Isabella de Bari, and Isabella Pisano. Syngas derived from lignocellulosic biomass gasification as an alternative resource for innovative bioprocesses. *Processes*, 8(12), 2020.

[19] Craig A. Grimes, Oomman K. Varghese, and Sudhir Ranjan. *Photoelectrolysis*, pages 115–190. Springer US, Boston, MA, 2008.

[20] Hao Ming Chen, Chih Kai Chen, RuXi Liu, Lei Zhang, Jiujun Zhang, and David P. Wilkinson. Nano-architecture and material designs for water splitting photoelectrodes. *Chemical Society reviews*, 41 17:5654–71, 2012.

[21] Paris IEA. Global hydrogen review 2023. 2023.

[22] European Commission. A hydrogen strategy for a climate-neutral europe, 2020.

[23] Ana-Maria Nasture et al. Energy storage systems: From classic to hydrogen. pages 105–138, 2021.

[24] REN21. *Renewables Global Futures Report: Great Debates Towards 100% Renewable Energy*. REN21 Secretariat, Paris, 2017.

[25] Étienne Rivard, Michel L. Trudeau, and K. Zaghib. Hydrogen storage for mobility: A review. *Materials*, 12, 2019.

[26] Test Driver. Stoccaggio dell'idrogeno a bordo dei veicoli. `https://test-driver.it/stoccaggio-dellidrogeno-a-bordo-dei-veicoli/`, Inserire l'anno. Accesso in data: Inserire la data di accesso.

[27] Qiwen Lai, Mark Paskevicius, Drew A. Sheppard, Craig E. Buckley, Aaron W. Thornton, Matthew R. Hill, Qinfen Gu, Jianfeng Mao, Zhenguo Huang, Hua Kun Liu, Zaiping Guo, Amitava Banerjee, Sudip Chakraborty, Rajeev Ahuja, and Kondo-Francois Aguey-Zinsou. Hydrogen storage materials for mobile and stationary applications: Current state of the art. *ChemSusChem*, 8(17):2789–2825, 2015.

[28] A. F. Kloutse, R. Zacharia, D. Cossement, R. Chahine, R. Balderas-Xicohténcatl, H. Oh, B. Streppel, M. Schlichtenmayer, and M. Hirscher. Isosteric heat of hydrogen adsorption on mofs: comparison between adsorption calorimetry, sorption isosteric method, and analytical models. *Applied Physics A*, 121(4):1417–1424, 2015.

[29] Saba Niaz, Taniya Manzoor, and Altaf Hussain Pandith. Hydrogen storage: Materials, methods and perspectives. *Renewable and Sustainable Energy Reviews*, 50:457–469, 2015.

[30] C. Lang, Y. Jia, X. Yan, L. Ouyang, M. Zhu, and X. Yao. Molecular chemisorption: a new conceptual paradigm for hydrogen storage. *Chem Synth*, 2:1, 2022.

[31] Elena Rozzi, Francesco Demetrio Minuto, and Andrea Lanzini. Dynamic modeling and thermal management of a power-to-power system with hydrogen storage in microporous adsorbent materials. *Journal of Energy Storage*, 41:102953, 2021.

[32] Peng Peng, Aikaterini Anastasopoulou, Kriston Brooks, Hiroyasu Furukawa, Mark E. Bowden, Jeffrey R. Long, Tom Autrey, and Hanna Breunig. Cost and potential of metal–organic frameworks for hydrogen back-up power supply. *Nature Energy*, 7(5):448–458, 2022.

[33] R.K. Ahluwalia and J.K. Peng. Automotive hydrogen storage system using cryo-adsorption on activated carbon. *International Journal of Hydrogen Energy*, 34(13):5476–5487, 2009.

[34] Inc. Toray Composite Material America. T700s standard modulus carbon fiber. Technical report.

[35] Vladimír Zeleňák and Ivan Saldan. Factors affecting hydrogen adsorption in metal-organic frameworks: A short review. *Nanomaterials (Basel)*, 11(7):1638, 2021.

[36] Maryam Kamal Kandezi, Vahid Sokhanvaran, Zohreh Ahadi, Nematollah Arshadi, Behzad Haghighi, Khashayar Ghandi, and Muhammad Shadman Lakmehsari. Hydrogen adsorption on methyl-functionalized irmof-1 and irmof-18 by molecular simulation. *Theoretical Chemistry Accounts*, 142(2):16, 2023.

[37] William L. Luyben. Estimating refrigeration costs at cryogenic temperatures. *Computers Chemical Engineering*, 103:144–150, 2017.

[38] J.H. Derking, H.J.M. ter Brake, A. Sirbi, M. Linder, and H. Rogalla. Optimization of the working fluid in a joule–thomson cold stage. *Cryogenics*, 49(3):151–157, 2009.

[39] S.S. Mohammadshahi, E.MacA. Gray, and C.J. Webb. A review of mathematical modelling of metal-hydride systems for hydrogen storage applications. *International Journal of Hydrogen Energy*, 41(5):3470–3484, 2016.

[40] L. Scott Blankenship, Norah Balahmar, and Robert Mokaya. Oxygen-

rich microporous carbons with exceptional hydrogen storage capacity. *Nature Communications*, 8(1):1545, 2017.